AD_____

Award Number:
W81XWH-10-1-0146

TITLE:
Oxidative Lung Injury in Virus-Induced Wheezing

PRINCIPAL INVESTIGATOR:
Roberto P. Garofalo, M.D.

CONTRACTING ORGANIZATION:
The University of Texas Medical Branch at Galveston
Galveston, TX 77555-5302

REPORT DATE:
May, 2014

TYPE OF REPORT:
Annual

PREPARED FOR:
U.S. Army Medical Research and Materiel Command
Fort Detrick, Maryland 21702-5012

REPORT DOCUMENTATION PAGE

Form Approved
OMB No. 0704-0188

1. REPORT DATE	2. REPORT TYPE	3. DATES COVERED
May 2014	Annual	1May2013 - 30Apr2014

4. TITLE AND SUBTITLE

Oxidative Lung Injury in Virus-Induced Wheezing

5a. CONTRACT NUMBER
W81XWH-10-1-0146

5b. GRANT NUMBER

5c. PROGRAM ELEMENT NUMBER

6. AUTHOR(S)

Roberto P. Garofalo, M.D.

E-Mail: rpgarofa@utmb.edu

5d. PROJECT NUMBER

5e. TASK NUMBER

5f. WORK UNIT NUMBER

7. PERFORMING ORGANIZATION NAME(S) AND ADDRESS(ES)
University of Texas Medical Branch at Galveston

Galveston, TX 77555-0372

8. PERFORMING ORGANIZATION REPORT NUMBER

9. SPONSORING / MONITORING AGENCY NAME(S) AND ADDRESS(ES)

U.S. Army Medical Research and Material Command

Fort Detrick, Maryland 21702-5012

10. SPONSOR/MONITOR'S ACRONYM(S)

11. SPONSOR/MONITOR'S REPORT NUMBER(S)

12. DISTRIBUTION / AVAILABILITY STATEMENT
Approved for Public Release; Distribution Unlimited

13. SUPPLEMENTARY NOTES

14. ABSTRACT

Over the past year we have focused on the role of the transcription factor Nrf2 in controlling expression of antioxidant genes in the lung of RSV-infected mice. In particular, we have shown that an Nrf2-inducing agent, BHA, can restore in part expression of the antioxidant genes SOD1 and catalase following RSV infection. We have also established a colony of Nrf2 KO mice and shown that lack of this transcription factor results in enhanced airway disease and viral replication in the lung. We have also identified a new strategy to increase level of Nrf2 expression in the lung by the use of adenovirus-associated vector 2 (AAV2). We have also initiated a fast backcross breeding protocol to generate Nrf2 KO mice in the BALB/c strain. We continue enrolling children with viral bronchiolitis and have validated a new FDA-approved Luminex xTAG Respiratory Viral Panel for the identification of co-infections and their role in mediating oxidative injury in infants. This panel has been designed to simultaneously probe for 12 viral targets in a single patient specimen (RSV/A, RSV/B, Influenza A, Influenza A subtype H1, Influenza A subtype H3, Influenza B, PIV-1, PIV-2, PIV-3, hMPV, Rhinovirus, and Adenovirus). We have published a peer-reviewed paper in the Am J Physiology and a comprehensive review in Antioxidant & Redox Signaling. Some of the data have been presented at the ESPID meeting in Milan, Italy.

15. SUBJECT TERMS Nothing Listed

16. SECURITY CLASSIFICATION OF:			17. LIMITATION OF ABSTRACT	18. NUMBER OF PAGES	19a. NAME OF RESPONSIBLE PERSON
a. REPORT	b. ABSTRACT	c. THIS PAGE			USAMRMC
U	U	U	UU	96	19b. TELEPHONE NUMBER *(include area code)*

Table of Contents

Page

Introduction……1

I. Body……1-6

II. Key Research Accomplishments…….. 6-11

III. Reportable Outcomes……..11-12

IV. Conclusion…… 12-13

V. References……..13-14

VI. Appendices……15-93

1. Komaravelli, N, Tian, B., Ivanciuc, T., Mautemps, N., Brasier, A.R., Garofalo, R.P., Casola, A. Respiratory Syncytial Virus Infection Downregulates Antioxidant Enzyme Expression by Triggering Deacetylation-Proteasomal Degradation of Nrf2. Free Radical Biology and Medicine, Special Issue, 2015 (submitted).
2. Li, H., Ma, Y., Ivanciuc, T., Komaravelli, N., Kelley, J.P., Ciro, C., Szabo, C., Garofalo, R.P., Casola, A. Role of Hydrogen Sulfide in Paramyxovirus Infections. Journal of Virology, 2015 (submitted).

.

Annual Progress Report for the period ending April 2014

INTRODUCTION

This project is in response to the Department of Defense Congressionally Directed Medical Research Programs, Investigator-Initiated Research Award and is addressing the topic area "Childhood asthma". The project focuses on respiratory syncytial virus (RSV), the single most important pathogen causing acute respiratory-tract infections in children. RSV infections are a major precipitating factor of wheezing in asthmatic children and have been linked to both the development and the severity of asthma. Our group has established a multidisciplinary and highly integrated pre-clinical and translational research program that focuses on the role of oxidative injury in the pathogenesis of severe RSV infections. We have discovered that in the course of RSV infections reactive oxygen species (ROS) are rapidly generated along with viral-mediated inhibition of protective antioxidant enzyme (AOE) genes in the lung. Thus, we propose a new molecular pathway by which respiratory viruses induce lung inflammation, with implication for novel therapeutic strategies of lower respiratory infections and virus-triggered precipitation of asthma attacks.

I. BODY

Statement of Work

This project is in response to the Department of Defense Congressionally Directed Medical Research Programs, Investigator-Initiated Research Award and is addressing the topic area "Childhood asthma". The project focuses on respiratory syncytial virus (RSV), the single most important pathogen causing acute respiratory-tract infections in children. RSV infections are a major precipitating factor of wheezing in asthmatic children and have been linked to both the development and the severity of asthma. Our group has established a multidisciplinary and highly integrated pre-clinical and translational research program that focuses on the role of oxidative injury in the pathogenesis of severe RSV infections. We have discovered that in the course of RSV infections reactive oxygen species (ROS) are rapidly generated along with viral-mediated inhibition of protective antioxidant enzyme (AOE) genes in the lung. Thus, we propose a new molecular pathway by which respiratory viruses induce lung inflammation, with implication for novel therapeutic strategies of lower respiratory infections and virus-triggered precipitation of asthma attacks. The scope of our work is summarized below.

Specific Aim 1 - To determine the mechanism(s) of inhibition of AOE expression in the lung during the course of RSV infection by dissecting the role of Nrf-mediated transcription pathways.

Aim 1a – Establish expression profile, kinetics and cellular source of AOE in mouse lung.

Task # 1. Perform WB analysis of AOE in lung tissue and BAL* (Year 1, Q1-2*).

Task # 1a. Submit amendment to IACUC protocol # 9001002A to cover experiments in Aim 1 and 2. **(Year 1, Q1-2)**

Milestone # 1. Approval of amendment(s) to IACUC protocol. (Year 1, Q1)

Task # 1b. Experiment 1: RSV or sham infection of BALB/c mice (total 80 animals) and extraction of lung and BAL proteins at different time points (day 1, 3, 5, 7, 9, 15, 21). **(Year 1, Q1-2)**

Task # 1c. Perform WB of normalized lung and BAL proteins with specific antibodies for AOE. **(Year 1, Q1-2)**

Task # 1d. Analysis and quantification of WB results. **(Year 1, Q1-2)**

Task # 1e. Experiment 2: repeat experiment in 1a-d (80 animals). Statistical analysis of AOE expression in RSV-infected vs sham-infected (control) lungs. **(Year 1, Q1-2)**

Completed

Milestone # 2. Complete quantitative kinetics of AOE protein expression in the lung/BAL after infection – 5 animal/each time point/each condition X 2 independent experiments. (Year 1, Q2)

***Task #2. Perform real time PCR analysis of AOE in lung tissue and BAL cells.* (Year 1, Q2-3)**

Task # 2a. Experiment 1: RSV or sham infection of BALB/c mice (total 80 animals) and extraction of lung and BAL cell RNA (day 1, 3, 5, 7, 9, 15, 21). **(Year 1, Q2-3)**

Task # 2b. Perform real time PCR of lung and BAL RNA with specific muse primers for AOE. **(Year 1, Q2-3)**

Task # 2c. Analysis and quantification of real time PCR results. **(Year 1, Q2-3)**

Task # 2d. Experiment 2: repeat experiment in 2a-c (80 animals) – Statistical analysis. **(Year 1, Q2-3)**

Completed

Milestone # 3. Complete quantitative kinetics of AOE mRNA in the lung/BAL cells after infection – 5 animal/each time point/each condition X 2 independent experiments. (Year 1, Q3)

***Task # 3. Identification of lung cells involved in RSV-mediated AOE modulation.* (Year 1, Q3-4)**

Task # 3a. Refine methodology to isolate total proteins from epithelial cells of the distant airways and alveolar macrophages. **(Year 1, Q3-4)**

Completed

Milestone # 4. Obtain > 90% cell-specific proteins from either distal airway epithelial cells or alveolar macrophages. (Year 1, Q4)

Task 3b. Experiment 1: based on results in Task # 1, infect mice and obtain epithelial and macrophage proteins at three to four representative time points (30-40 animals). **(Year 1, Q4)**

Task # 3c. Perform WB analysis of cell proteins with specific antibodies for AOE enzymes. **(Year 1, Q4)**

Task # 3d. Experiment 2: repeat experiment in 3b-c (30-40 animals). Statistical analysis. **(Year 1, Q-4)**

Completed

Milestone # 5. Complete analysis of specific cell source of AOE during RSV infection and its expression pattern. (Year 1, Q4)

Aim 1b – Activation of Nrf2 and Nrf3 in the lung of RSV-infected mice.

Task # 4 – Perform WB and EMSA analysis of lung and BAL nuclear proteins. **(Year 1, Q3-4)**

Task # 4a. Experiment 1: RSV or sham infection of BALB/c mice (total 80 animals) and extraction of lung and BAL nuclear proteins (day 1, 3, 5, 7, 9, 15, 21). **(Year 1, Q3-4)**

Task # 4b. WB of normalized nuclear lung and BAL proteins with specific antibodies for Nrf2 and Nrf3. Analysis and quantification. **(Year 1, Q3-4)**

Task # 4c. EMSA of normalized nuclear lung and BAL proteins with specific Nrf2 and Nrf3 DNA-binding sequences. Analysis and quantification. **(Year 1, Q3-4)**

Task # 4d. Experiment 2: repeat experiment in 4a-c (80 animals). Statistical analysis. **(Year 1, Q3-4)**

Completed (in progress protein analysis, see below)

Milestone # 6. Complete analysis of RSV-mediated inhibition and/or activation of Nrf2 and Nrf3 as critical regulatory elements of AOE transcriptional activity. (Year 1, Q4)

Completed

Specific Aim 2 - To establish whether pharmacologic intervention aimed to increase Nrf2 activation in the airways or to supplement the antioxidant response via synthetic antioxidant mimetics results in protection from viral-induced lung injury and clinical disease.

Aim 2a – Effect of activation of Nrf2-dependent AOE expression by synthetic triterpenoids on RSV-induced lung oxidative injury and clinical disease.

Task # 5. Establish appropriate treatment of mice with triterpenoids (CDDO) that results in increased Nrf2 activation in the lung and AOE expression. **(Year 2, Q1-2)**

Task # 5a. Treatment of groups of BALB/c mice with the synthetic triterpenoid CDDO to establish proper pharmacologic dose (two i.p. doses, three groups of mice, including one group treated with control vehicle, total 150 mice) – Lung nuclear protein extraction five days after initial dose. Potential drug toxicity monitored by daily body weight assessment. **(Year 2, Q1-2)**

Task # 5b. WB and EMSA of nuclear lung proteins with specific antibodies for Nrf2 as in Task # 4b-c. Analysis and quantification comparing CDDO-treated vs vehicle-treated mice. **(Year 2, Q1-2)**

Task # 5c. Treatment of BALB/c mice with dose and schedule of CDDO established in task # 5a-b. Extraction of total lung proteins for assessment of AOE expression by WB and/or real time PCR
(total 100 mice). Repeat experiment twice. **(Year 2, Q2)**

Completed (*we have employed BHA and AOE mimetics since CDDO had toxicity*)

Milestone # 7. Establish dose and schedule of CDDO that result in Nrf2 activation and AOE expression in lung of BALB/c mice. (Year 2, Q2)

***Task # 6. Effect of CDDO treatment on RSV-induced clinical disease, AHR and oxidative damage in the lung*. (Year 2, Q2-3)**

Task # 6a. RSV infection of CDDO-treated or vehicle-treated (control) BALB/c mice and determination of clinical disease by body weight loss, clinical disease score, and AHR by Buxco, over 21 days (50 animals total). Peak viral replication will be determined at day 5. Experiment will be repeated twice. Statistical analysis. **(Year 2, Q2-3)**

Task # 6b. RSV infection of CDDO-treated or vehicle-treated (control) BALB/c mice and analysis of lung and BAL for lipid peroxidation markers (MDA and 4-HNE) and for measurement of 8-isoprostane (total 50 mice). Experiment will be repeated twice. Statistical analysis. **(Year 2, Q2-3)**

Completed (*we have employed BHA and AOE mimetics*)

Milestone # 8. Complete determination of protective effect of triterpenoids on RSV-induced clinical disease and oxidative damage in a mouse model. (Year 2, Q3)

Aim 2b – Effect of catalytic scavengers on RSV-induced lung oxidative injury and clinical disease.

Task # 7. *Effect of synthetic SOD and catalase mimetics on RSV-induced clinical disease and AHR*. (Year 2, Q3-4)

Task # 7a. Mice treated with the mimetics EUK-8 or EUK-134 or with vehicle control by gavage. Dose and schedule treatment will be established based on published data by scientists who developed these compounds and experience by the PI with the anti-oxidant BHA. Anticipated need for 200 mice to set up conditions. Potential toxicity will be monitored by body weight loss. **(Year 2, Q3-4)**

Task # 7b. RSV infection of EUK-treated or vehicle-treated (control) BALB/c mice and determination of clinical disease by body weight loss, clinical disease score, and AHR by Buxco, over 21 days (100 animals total). Peak viral replication will be determined at day 5. Experiment will be repeated twice. Statistical analysis. **(Year 2, Q3-4)**

Completed (in progress 2D gel analysis, see below)

Milestone # 9. Complete determination of protective effect of synthetic SOD and catalase mimetics on RSV-induced clinical disease and AHR in a murine model. (Year 2, Q4)

Completed

Overall, for Aim 1 and Aim 2 (mouse model) we are performing analysis of BAL and lung proteins generated by 2DE gels (several hundreds protein spots).

Aim 3 - Analyze whether distinct AOE expression patterns at the airway mucosal site can discriminate between infants with different severity of illness and/or degree of oxidative-associated injury following naturally-acquired RSV infection.

Aim 3a – Expression of AOE and oxidative stress markers in NPS of RSV-infected infants.

***Task # 8. Perform WB for AOE in NPS of RSV-infected infants that were previously collected.* (Year 2, Q1-2)**

Task # 8a. Submit amendment to IRB protocol # 03-117: addition of new investigators and scope of the work covered in this grant. **(Year 1, Q1)**

Completed

Milestone # 10. Approval of amendment(s) to IRB protocol. (Year 1, Q1)

Task # 8b. Set up conditions for WB of AOE in NPS, including clean-up of mucus from samples, amount of protein, concentration of primary antibodies, secondary antibody. Set up conditions for measurement of lipid peroxidation markers (MDA and 4-HNE) and for measurement of 8-isoprostane. **(Year 2, Q1-2)**

Task # 8c. Perform WB for AOE and oxidative marker assays in 150 previously collected and stored (- 70^0 C) samples of NPS from RSV-infected infants. **(Year 2, Q1-2)**

Task # 8d. Analysis and quantification of WB results. **(Year 2, Q1-2)**

Completed

Milestone # 11. Complete analysis of AOE in stored samples of human NPS collected from RSV infections. (Year 2, Q2)

Task # 9. Analysis of AOE, protein patterns, and oxidative markers in prospectively enrolled infants with different clinical severity of RSV infection.

Task # 9a. Enroll infants and young children with RSV infections, URTI or LRTI (bronchiolitis, with or without hypoxemia). Enrollment on the ward, outpatient clinic, or emergency room. Collect NPS samples for virus identification, protein analysis. Collect clinical data. **(Year 1, Q2-4;Year 2, Q1-4;Year 3,1-2)**

Task # 9b. Perform WB for AOE and assays for MDA, 4-HNE, and 8-isoprostane in samples of NPS (total samples over 3 year study ~ 200). **(Year 2, Q1-4; Year 3, Q1-2)**

Task # 9c. Analysis and quantification of WB and other assays, statistical analysis and correlation with clinical severity, other parameters of infection. **(Year 3, Q2)**

In Progress – Analysis of protein results

Milestone # 12. Assessment of AOE and oxidative markers in NPS and their relationship to disease severity in RSV-infected infants. (Year 3, Q3)

Aim 3b – Differential protein expression in fractionated NPS samples by 2DE and MALDI/TOF/TOF.

***Task # 10. Set up conditions for NPS fractionation and subsequently analysis by 2DE gels or Electrospray MS/MS.* (Year 2, Q1)**

Task # 10a. NPS fractionation by size exclusion chromatography (SEC) and 2DE gels of proteins with MW > 26kDA: set up conditions using previously collected and stored (- 70^0 C) samples of NPS from RSV-infected infants. Run samples in duplicate. **(Year 1, Q4; Year 2, Q1-4, Year 3, Q1)**

Task # 10b. Trypsin digestion and Electrospray MS/MS of protein fractions < 26 kDA - Run sample in duplicate. **(Year 2, Q2-4; Year 3, Q1)**

In Progress – Analysis of MALDI-TOF peaks

Milestone # 13. Establish a reproducible methodology to fractionate proteins in NPS by SEC.

Task # 11. Identify differential expressed proteins in fractionated NPS from infants with URTI or bronchiolitis. **(Year 3, Q1)**

Task # 11a. Perform mass fingerprinting of prospectively collected NPS by MALDI-TOF and MS of proteins and a Bayesian statistical algorithm. **(Year 3, Q3)**

Task # 11b. Sequencing of selected proteins by LC/MS/MS **(Year 3, Q4)**

In Progress – Analysis of MALDI-TOF peaks

Milestone # 14. Build a map of NPS proteins that are quantitatively or functionally associated with more severe manifestations of RSV infections. (Year 3, Q4)

In Progress – Analysis of NPS proteome by Ingenuity pathway

II. KEY RESEARCH ACCOMPLISHMENTS

Hypothesis

Respiratory syncytial virus (RSV) is the single most important virus causing acute respiratory-tract infections in children and is a major cause of severe respiratory morbidity and mortality in elderly (Hall 1917-28). Overall, the World Health Organization estimates that RSV is responsible for 64 million clinical infections and 160 thousand deaths annually worldwide (Falsey et al. 1749-59). In addition to acute morbidity, RSV infections have been linked to both the development and the severity of asthma. We have shown that ROS are involved in the signaling transduction pathways that control inducible expression of chemokine and other inflammatory genes in response to RSV infection, yet blocking ROS production does not significantly increase viral replication in the lung and even decreases viral replication in cells (Casola et al. 19715-22;Liu et al. 2461-69;Liu et al.;Castro et al. 1361-69). Recently, in the course of proteomics studies aimed to profile global protein expression we made two important discoveries: 1) RSV potently inhibits the expression of antioxidant enzyme (AOE) genes, including Glutathione S-transferases (GST), Superoxide dismutases (SOD) and catalase; 2) following RSV infection, expression of nuclear NF-E2 related factor-2 (Nrf2), which positively regulates basal and inducible expression of AOE genes is downregulated both in cells and in the lung (Jaiswal 1199-207), while Nrf3 which negatively regulates AOE gene expression (Sankaranarayanan and Jaiswal 50810-17) is induced in epithelial cells. **Our general hypothesis is that ROS production along with the inhibition of cytoprotective AOE expression lead to severe manifestations of RSV infection.**

Specific Aims

Specific Aim 1 - To determine the mechanism(s) of inhibition of AOE expression in the lung during the course of RSV infection by investigating the role of Nrf-dependent gene transcription. Using a well characterized murine model of experimental infection we will establish by real-time PCR and WB the expression profile,

kinetics and cellular source of AOE in the lung over a period of 21 days following RSV inoculation (**1a**). To test our novel hypothesis that RSV inhibits AOE gene transcription by inhibiting Nrf2 expression and/or activating Nrf3 we will perform WB and EMSA studies of total lung or cell-specific nuclear proteins (**1b**).

Specific Aim 2 - To establish whether pharmacologic intervention aimed to increase Nrf2 activation in the airways or to supplement the antioxidant response via synthetic antioxidant mimetics results in protection from viral-induced lung injury and clinical disease. We will test the specific hypothesis that increasing the lung/airway antioxidant capacity, either by activating Nrf-2-ARE-mediated expression of endogenous AOE genes (**2a**) or by providing exogenous synthetic antioxidants mimetics (**2b**) may be used as a pharmacologic strategy to treat RSV infections. Using the murine model we will determine by established clinical-like parameters and pathophysiologic endpoints of airway dysfunction the effect of such pharmacologic treatments on experimental RSV infection. Markers of oxidation and oxidative-associated injury will be used as correlates of protection following treatment with Nrf-2 modulating compounds or antioxidants mimetics.

Specific Aim 3 – To analyze whether distinct AOE expression profile at the airway mucosal site can discriminate between infants with different severity of illness and/or degree of oxidative-associated injury following naturally-acquired RSV infections. In **3a**, the profile and relative abundance of AOE proteins present in nasopharyngeal secretions (NPS) collected from infants with RSV infections of different clinical severity will be analyzed by Western blots. NPS will be also tested for a panel of oxidative stress markers, including the lipid peroxidation products 8-isoprostane, malonaldehyde (MDA) and 4-hydrynonenal (4-HNE). In **3b,** we will apply our novel biofluids fractionation platform to analyze the NPS proteome by high resolution two-dimensional gel electrophoresis (2DE), and MALDI-TOF/TOF mass spectroscopy. These studies will determine whether viral-mediated inhibition of AOE expression, which we discovered in epithelial cells and - in preliminary experiments - in mouse lung, is associated with the most severe clinical manifestations of RSV infection in children, thus contributing to oxidative injury in the airways.

- Since the last report we have made major progress towards our goal of increasing lung Nrf2 expression levels in the lung by using recombinant replication-deficient adenovirus gene transfer in RSV-infected mice. In collaboration with Dr. Sergei Atamas at University of Maryland, Baltimore, we have generated a recombinant replication-deficient adenovirus (AdV) expressing murine Nrf2, using the RAPAd system described elsewhere in details [Vira-Quest, North Liberty, IA) (Anderson et al. 1034-38)]. The resultant purified adenovirus vector has a concentration of $0.9X10^{12}$ particles/ml and an infectious titer of $4X10^{10}$ plaque-forming units (PFU)/ml and was termed AdV-mNrf2. Control adenovirus vector AdV-Null with no insert in the E1 region was produced in the same manner. Both vectors have green fluorescent protein (GFP)-encoding gene inserts in the E3 region, to permit detection in the lung by green fluorescence. Dr. Atamas has previously shown that this strategy using AdV encoding proteins and cytokines results in high level of functional expression of the foreign gene product in the lung following intratracheal instillation (Luzina et al. 999-1008;Luzina et al. 1530-39;Pochetuhen et al. 428-37). In preliminary experiments performed in BALB/c mice we have shown peak expression of GFP in the lung at 5 days after either intratracheal or intranasal instillation

of the AdV constructs at a range from 1 to $5X10^8$ PFU/mouse. Importantly, we have shown that the replication-deficient AdV *per se* does not affect the subsequent infection with RSV in terms of viral replication or disease. Nrf2 levels will be investigated by WB analysis in lung nuclear extracts. Conditions shown to be optimal for Nrf2 expression will be used to investigate RSV lung titers (as primary endpoint) at different days post-inoculation (day 1, 3, 5, 7) and other parameters of RSV-induced oxidative injury and lung disease, as described (Castro et al. 1361-69;Hosakote et al. 1550-60). Experiments will cover a range of age at the time of infection from neonate mice (4 days) to adults 8-10 weeks. New findings related to the regulation of lung Nrf2 have been submitted for publication (please see **Appendix 1**).

- As part of our effort to identify key proteins and enzymes that are involved in the biosynthesis of reactive oxygen species we have discovered a new critical endogenous pathway that is involved in viral replication. This pathway regulates the generation and catabolism of hydrogen sulfide (H_2S). For several hundred years, H_2S has been known to exist in animal tissues as a noxious gas. As H_2S is typically formed by commensal bacteria, it was not regarded as physiologically significant. However, recent studies have established that H_2S is indeed a biologically relevant signaling molecule in mammals [reviewed in (Paul and Snyder 499-507)]. H_2S acts as a messenger molecule, and together with the volatile substances nitric oxide (NO) and carbon monoxide (CO) it is defined as a gasotransmitter, playing physiological roles in a variety of functions such as synaptic transmission, vascular tone, angiogenesis, inflammation and cellular signaling (Chen and Wang 130-38). The generation of H_2S is catalysed by cystathionine β-synthase (CBS), cystathionine γ-lyase (CSE) and 3-mercaptopyruvate sulfurtransferase (MST)(**Fig.1**). Homocysteine, derived from Met, is condensed with Ser by CBS to generate cystathionine, which is converted to Cys by CSE. This Cys is used as a substrate for both CBS and CSE to produce H_2S. The expression of CBS and CSE, have the key enzymes responsible for H_2S generation, is tissue-specific with CBS being expressed predominantly in the brain and CSE in peripheral tissues, including lung. CSE expression and activity are developmentally regulated as demonstrated by studies in premature infants, newborns and infants in the first year of life, in which this enzyme has been measured and found to be delayed in

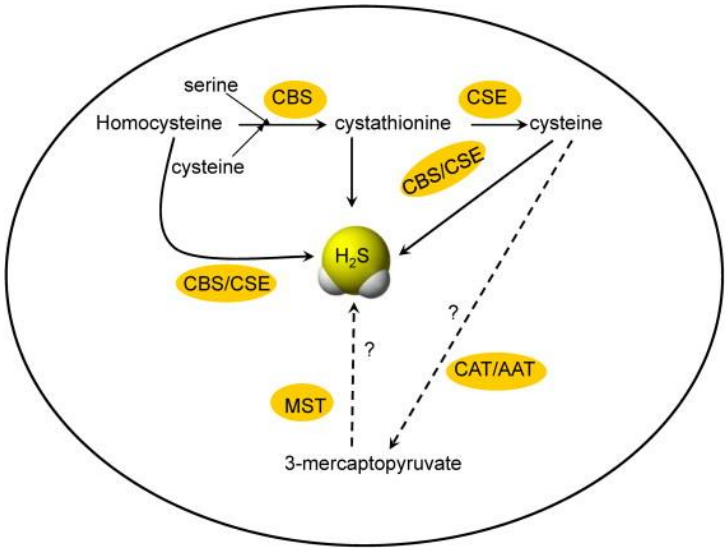

Fig. 1 Metabolic pathways for endogenous produced H_2S. (*adapted from Chen Y, Respir Physiol & Neurobiol, 184;130-134, 2012*). H_2S is produced endogenously in mammals including humans. Two cytoplasmic enzymes, cystathionine-γ-lyase (CSE) and cystathionine-β-synthase (CBS) are responsible for H_2S biogenesis. MST catalyzes the formation of H_2S from 3-mercaptopuruvate, a cysteine metabolite. CAT/AAT is an aminotransferase, which can catalyse the conversion of cysteine to 3-mercaptopuruvate. Whether CAT/AAT and MST actually produce H_2S in the respiratory have been uncertain.

maturation (Vina et al. 1067-69) (Zlotkin and Anderson 65-68). CSE-deficient mice exhibit a profound depletion of H_2S in peripheral tissues (Yang et al. 587-90). Recently, a third potential enzymatic mode of H_2S formation involving the enzyme MST has been posited, but evidence for its involvement in the physiological biosynthesis of H_2S in mammals is as yet weak. In the respiratory tract, endogenous H_2S has been shown to participate in the regulation of important physiological functions such as airway tone, pulmonary circulation, cell proliferation or apoptosis, fibrosis, oxidative stress, and inflammation (Chen and Wang 130-38). Reduced levels of serum H_2S in patients with COPD has been reported (Chen et al. 3205-11) and in a rat model of chronic cigarette smoke (CS)-induced COPD endogenous H_2S plays a protective role as anti-inflammatory and bronchodilator mediator (Chen et al. 334-41). Moreover, peritoneal administration of the H_2S donor sodium hydrosulfide (NaHS) to CS-exposed rats alleviated airway hyperreactivity (AHR), decreased lung pathology as well as the levels of IL-8 and TNF-α in lung tissue. Han et al. have shown similar results in a mouse model of tobacco smoke (TS)-induced emphysema (Han et al. 2121-34). In that study, TS exposure for 12 and 24 weeks reduced the protein contents of CSE and CBS in the lungs. TS-induced emphysema, thickness of bronchial walls, and cellular inflammation in bronchial alveolar lavage (BAL) were all ameliorated by NaHS-mediated H_2S synthesis.

- There are no studies investigating the role of H_2S generation in pathophysiology of viral infections or the use of H_2S donors as pharmacological intervention for viral-induced airway diseases. Recently, our laboratory has made critical discoveries that are the rationale for the studies proposed in this application and are presented in the **Appendix 2** (manuscript submitted) and in the following preliminary results (**Figs. 2-4**). Using an *in vitro* model of RSV infection of airway epithelial cells, we demonstrated that: 1) RSV infection inhibited expression of the CSE enzyme, reduced ability to generate cellular H_2S, and increased H_2S degradation; 2) Inhibition of H_2S generation, using propargylglycine (PAG), an inhibitor of CSE, was associated with increased production of virus infectious particles, as well as increased secretion of proinflammatory cytokines; 3) Treatment of both A549 (a lung carcinoma cell line retaining features of type II alveolar epithelial cells) and primary small alveolar epithelial (SAE) cells with GYY4137 (morpholin-4-ium 4 methoxyphenyl(morpholino)phosphinodithioate), a slow-releasing H_2S compound, significantly inhibited viral replication at a step subsequent to viral adsorption. These findings are presented in details in Appendix 2. In addition, we found that genetic deficiency of CSE (using CSE -/- mice) resulted in increased airway hyperresponsiveness (AHR) in CSE -/- mice compared to WT controls, following either exposure to cigarette smoke or RSV infection (**Fig. 2, next page**). Moreover, we found that intranasal treatment of BALB/c mice with GYY4137 significantly attenuated disease following RSV infection and similarly to our findings in cells inhibited viral replication in the lung (**Fig. 3, next page).** GYY4137 treatment was also characterized by a blunted viral-induced neutrophilia in BAL and reduced AHR (**Fig. 4, next page**). <u>Overall, our studies have identified a previously unknown function of endogenous H_2S that may play a critical role in the pathogenesis of viral respiratory infections associated with exposure to SHTS</u>.

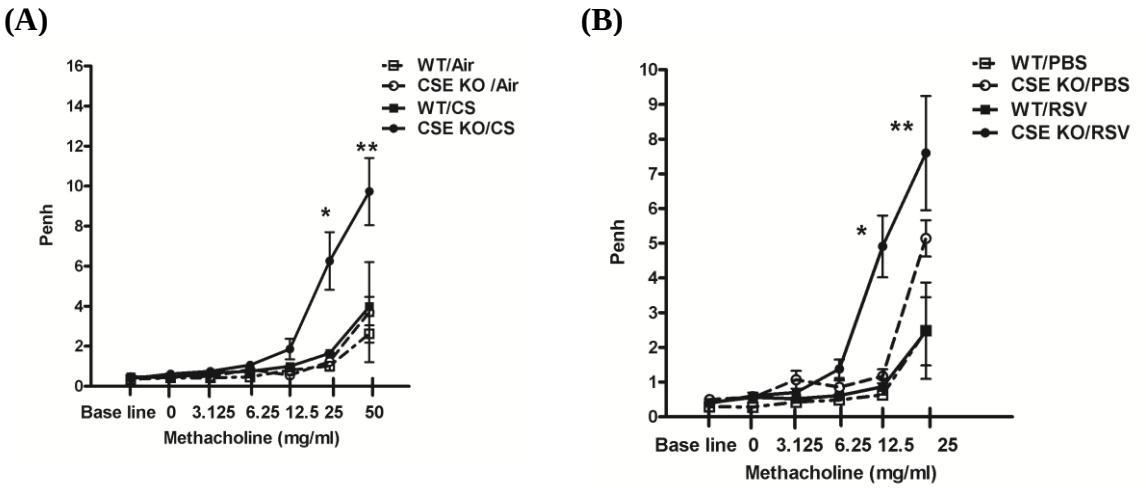

Fig. 2. CSE gene deficiency increases AHR in mice. (A) CSE gene deficiency increases AHR in mice exposed to cigarette smoke. WT and CSE -/- mice were exposed in a chamber to cigarette smoke (CS) of five cigarettes/ day (3R4F research cigarette from University of Kentucky) or air for 4 consecutive days. Unrestrained, whole-body plethysmography (Buxco Electronics, Inc. Sharon, CT) was used to measure the Enhanced Pause (Penh) to evaluate AHR. Baseline and post-methacholine challenge Penh values were determined after cigarette smoke or air exposure. Penh values are presented as mean ± SEM (n = 4 mice/group). * p<0.05 compared with WT/CS; ** p<0.01 compared with WT/CS. **(B)** CSE gene deficiency increases AHR following RSV infection. WT and CSE -/- mice were inoculated with either RSV dose 107 PFU or mock-infected. Baseline and post-methacholine challenge Penh values were determined at day 5 post-infection. Data are means ± SEM (n = 3-4 mice/group). * p<0.005 compared with WT/RSV; ** p<0.05 compared with WT/RSV.

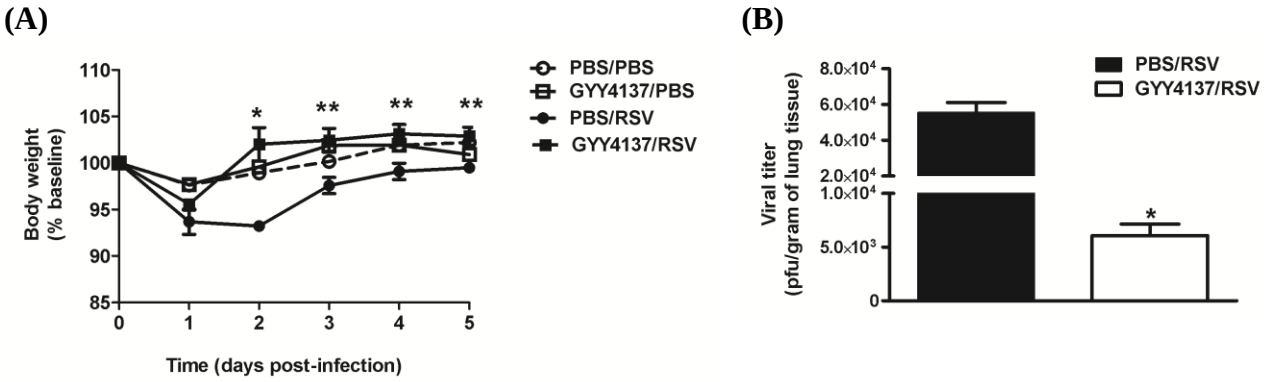

Fig. 3. H_2S donor treatment attenuates RSV-induced clinical disease and viral replication *in vivo*. (A) Disease parameters. Mice were treated i.n. with GYY4137 (50 mg/kg body weight) or an appropriate volume of vehicle (PBS) 1h before, 6h and 20h after infection. Mice were inoculated with RSV dose 10^6 PFU or mock-infected. Data are expressed as mean ± SEM (n = 4 mice/group) and is representative of two independent experiments. * p<0.01 compared with PBS/RSV at day 2 p.i., ** p<0.05 compared with PBS/RSV at days 3, 4, and 5 p.i. **(B)** Viral replication in the lungs. At day 5 p.i., lungs were excised and viral replication was determined by plaque assay. The bar graph represents mean ± SEM (n = 4 mice/group). * p<0.01 compared with PBS/RSV group.

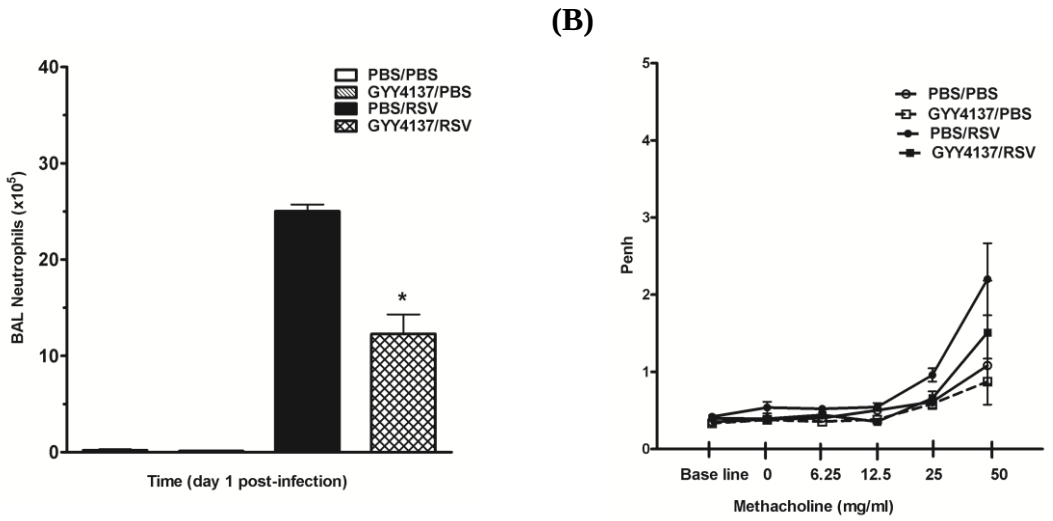

Fig. 4. Effect of H_2S donor on neutrophils populations in BAL and AHR in response to RSV infection. Mice were treated i.n. with GYY4137 (50 mg/kg body weight) or an appropriate volume of vehicle (PBS) 1h before, 6h and 20h after infection. Mice were inoculated with either RSV dose 10^6 PFU or mock-infected. **(A)** Neutrophils cell counts were determined in BAL samples at day 1 post-infection. Cell preparations were stained (Wright-Giemsa) and counted under the microscope (200 cells/slide). The bar graph represents mean ± SEM (n = 4 mice/group).*p<0.001 compared with PBS/RSV group. **(B)** Unrestrained, whole-body plethysmography (Buxco Electronics, Inc. Sharon, CT) was used to measure the Enhanced Pause (Penh) to evaluate AHR. Baseline and post-methacholine challenge Penh values were determined at day 5 post-infection. Penh values are presented as mean ± SEM (n = 4 mice/group).

III. REPORTABLE OUTCOMES

a. Manuscripts, abstracts, presentations:

1. Komaravelli, N, Tian, B., Ivanciuc, T., Mautemps, N., Brasier, A.R., Garofalo, R.P., Casola, A. Respiratory Syncytial Virus Infection Downregulates Antioxidant Enzyme Expression by Triggering Deacetylation-Proteasomal Degradation of Nrf2. Free Radical Biology and Medicine, Special Issue, 2015 (submitted).
2. Li, H., Ma, Y., Ivanciuc, T., Komaravelli, N., Kelley, J.P., Ciro, C., Szabo, C., Garofalo, R.P., Casola, A. Role of Hydrogen Sulfide in Paramyxovirus Infections. Journal of Virology, 2015 (submitted).

b. Licenses applied for and/or issued:

1. Provisional Patent

Casola A and Garofalo RP: Methods for Treating Viral Infections using Hydrogen Sulfide Donors. US Patent Number 62/006,680. Issued June 18, 2014.

c. Informatics such as databases and animal models, etc.:

1. We have generated a Nrf2-KO murine model of RSV infection. C57BL6J $Nrf2 +/-$ (strain name B6.129X1-Nfe2l2tm1Ywk/J) mice were purchased from Jackson laboratory. Nrf2-KO mice were generated by mating heterozygous female with homozygous male, and the offspring were genotyped. We are currently backcrossing this mouse to BALB/c.

d. Funding applied for based on work supported by this award:

1R21AI109099-01 (Garofalo) 09/01/13-08/31/15
NIH/NIAID
Antiviral Innate Pathways and Superoxide Dismutase in RSV Bronchiolitis
The goal of this project are to help provide a better understanding of the molecular mechanisms by which exposure to environmental tobacco smoke affects the severity of viral bronchiolitis in infants.

1R21AI103565-01 (Casola) 09/01/13-08/31/15
NIH/NIAID
A Novel Role of NF-κB in Viral-induced Airway Oxidative Stress

In this project we will pursue the hypothesis that NF-κB plays a key role in RSV-induced lung disease as it antagonizes Nrf2-dependent gene expression, leading to inhibition of airway antioxidant defenses and subsequent oxidative lung damage.

e. Employment or research opportunities applied for and/or received based on experience/training supported by this award:

1. Postdoctoral Fellow, Yashoda Hosakote, Ph.D., received a Young Clinical Scientist Award in 2013 from the Flight Medical Research Institute (FAMRI) entitled "Tobacco Smoke and HMGB1 in RSV Bronchiolitis".

IV. CONCLUSIONS

During this year of no cost-extension we continued to investigate mechanism that control antioxidant enzymes (AOE) in RSV infection. RSV infection in cells, mice and children leads to rapid generation of reactive oxygen species, which are associated with oxidative stress and lung damage, due to a significant decrease in the expression of airway AOEs. Oxidative stress plays an important role of in the pathogenesis of RSV-induced lung disease, as antioxidants ameliorate clinical disease and inflammation *in vivo*. We have generated a new model of the overexpression of Nrf2 in the lung via an AdV-driven approach. In addition, we have shown that RSV infection induces a progressive reduction in nuclear and total cellular level of Nrf2, resulting in decreased binding to endogenous AOE gene promoters and decreased AOE expression. RSV induces Nrf2 deacetylation and degradation via the proteasome pathway *in vitro and in vivo*. Histone deacetylase and proteasome inhibitors block Nrf2 degradation and increase Nrf2 binding to AOE

endogenous promoters, resulting in increased AOE expression. Known inducers of Nrf2 are able to increase Nrf2 activation and subsequent AOE expression during RSV infection *in vitro and in vivo*, with significant amelioration of oxidative stress. This is the first study to investigate the mechanism(s) of viral-induced inhibition of AOE expression. RSV-induced inhibition of Nrf2 activation, due to deacetylation and proteasomal degradation, could be targeted for therapeutic intervention aimed to increase antioxidant airway capacity during infection.

Searching for other oxidative-mediated mechanisms of RSV-induced disease we have discovered using slow-releasing H_2S donor GYY4137 and propargylglysin (PAG), an inhibitor of cystathionine-γ-lyase (CSE), a key enzyme that produce intracellular H_2S, that RSV infection led to reduced ability to generate and maintain intracellular H_2S levels in airway epithelial cells. Inhibition of CSE with PAG resulted in increased viral replication and chemokine secretion. On the other hand, treatment of epithelial cells with the H_2S donor GYY4137 reduced proinflammatory mediator production and significantly reduced viral replication, even when administered several hours after viral absorption. GYY4137 also significantly reduced replication and inflammatory chemokine production induced by human metapneumovirus (hMPV), suggesting a broad inhibitory effect of H_2S administration on paramyxovirus replication. GYY4137 treatment had no effect on RSV genome replication, viral mRNA and protein synthesis, indicating that the inhibition occurs at the level of assembly and/or cellular release. GYY4137 inhibition of proinflammatory gene expression occurred by modulation of activation of the key transcription factors Nuclear Factor (NF)-κB and Interferon Regulatory Factor (IRF)-3. Our results underscore an important role of H_2S in regulating virus infection and host defenses that could lead to a novel treatment strategy for RSV infection.

V. REFERENCES

Anderson, R. D., et al. "A simple method for the rapid generation of recombinant adenovirus vectors." Gene Ther. 7.12 (2000): 1034-38.

Casola, A., et al. "Oxidant tone regulates RANTES gene transcription in airway epithelial cells infected with Respiratory Syncytial Virus: role in viral-induced Interferon Regulatory Factor activation." J Biol Chem. 276 (2001): 19715-22.

Castro, S. M., et al. "Antioxidant Treatment Ameliorates Respiratory Syncytial Virus-induced Disease and Lung Inflammation." Am.J.Respir.Crit Care Med. 174.12 (2006): 1361-69.

Chen, Ya Hong, et al. "Involvement of endogenous hydrogen sulfide in cigarette smoke-induced changes in airway responsiveness and inflammation of rat lung." Cytokine 53.3 (2011): 334-41.

Chen, Ya Hong, et al. "ENdogenous hydrogen sulfide in patients with copd*." CHEST Journal 128.5 (2005): 3205-11.

Chen, Yahong and Rui Wang. "The message in the air: Hydrogen sulfide metabolism in chronic respiratory diseases." Respiratory Physiology & Neurobiology 184.2 (2012): 130-38.

Falsey, A. R., et al. "Respiratory syncytial virus infection in elderly and high-risk adults." N.Engl.J.Med. 352.17 (2005): 1749-59.

Hall, C. B. "Respiratory syncytial virus and parainfluenza virus." N.Engl.J Med. 344.25 (2001): 1917-28.
Han, W., et al. "Hydrogen sulfide ameliorates tobacco smoke-induced oxidative stress and emphysema in mice." Antioxid.Redox.Signal. 15.8 (2011): 2121-34.
Hosakote, Y. M., Jantzi, P. D., Esham, D. L., Spratt, H., Kurosky, A., Casola, A., and Garofalo, R. P. Viral-mediated inhibition of antioxidant enzymes contributes to the pathogenesis of severe respiratory syncytial virus bronchiolitis. Am J Respir Crit Care Med 183[1], 1550-60. 6-1-2011.
Ref Type: Journal (Full)
Jaiswal, A. K. "Nrf2 signaling in coordinated activation of antioxidant gene expression." Free Radic.Biol.Med. 36.10 (2004): 1199-207.
Liu, T., et al. "ROS mediate viral-induced stat activation: role of tyrosine phosphatases." J.Biol.Chem. (2003).
---. "Reactive oxygen species mediate virus-induced STAT activation: role of tyrosine phosphatases." J.Biol.Chem. 279.4 (2004): 2461-69.
Luzina, I. G., et al. "Interleukin-33 potentiates bleomycin-induced lung injury." Am.J.Respir.Cell Mol.Biol. 49.6 (2013): 999-1008.
Luzina, I. G., et al. "Regulation of pulmonary inflammation and fibrosis through expression of integrins alphaVbeta3 and alphaVbeta5 on pulmonary T lymphocytes." Arthritis Rheum. 60.5 (2009): 1530-39.
Paul, B. D. and S. H. Snyder. "H(2)S signalling through protein sulfhydration and beyond." Nat.Rev.Mol.Cell Biol. 13.8 (2012): 499-507.
Pochetuhen, K., et al. "Complex regulation of pulmonary inflammation and fibrosis by CCL18." Am.J.Pathol. 171.2 (2007): 428-37.
Sankaranarayanan, K. and A. K. Jaiswal. "Nrf3 negatively regulates antioxidant-response element-mediated expression and antioxidant induction of NAD(P)H:quinone oxidoreductase1 gene." J.Biol.Chem. 279.49 (2004): 50810-17.
Vina, J., et al. "L-cysteine and glutathione metabolism are impaired in premature infants due to cystathionase deficiency." Am.J.Clin.Nutr. 61.5 (1995): 1067-69.
Yang, G., et al. "H2S as a physiologic vasorelaxant: hypertension in mice with deletion of cystathionine gamma-lyase." Science 322.5901 (2008): 587-90.
Zlotkin, S. H. and G. H. Anderson. "The development of cystathionase activity during the first year of life." Pediatr.Res. 16.1 (1982): 65-68.

VI. APPENDIX

1. Komaravelli, N, Tian, B., Ivanciuc, T., Mautemps, N., Brasier, A.R., Garofalo, R.P., Casola, A. Respiratory Syncytial Virus Infection Downregulates Antioxidant Enzyme Expression by Triggering Deacetylation-Proteasomal Degradation of Nrf2. Free Radical Biology and Medicine, Special Issue, 2015 (submitted).
2. Li, H., Ma, Y., Ivanciuc, T., Komaravelli, N., Kelley, J.P., Ciro, C., Szabo, C., Garofalo, R.P., Casola, A. Role of Hydrogen Sulfide in Paramyxovirus Infections. Journal of Virology, 2015 (submitted).

ORIGINAL RESEARCH COMMUNICATION

RESPIRATORY SYNCYTIAL VIRUS INFECTION DOWNREGULATES ANTIOXIDANT ENZYME EXPRESSION BY TRIGGERING DEACETYLATION-PROTEASOMAL DEGRADATION OF NRF2

Narayana Komaravelli[1], Bing Tian[2], Teodora Ivanciuc[1], Nicholas Mautemps[1], Allan R. Brasier[2,3], Roberto P. Garofalo[1,3] , and Antonella Casola[1,3*]

Departments of Pediatrics[1], Internal Medicine[2], and Sealy Center for Molecular Medicine[3], University of Texas Medical Branch at Galveston, Texas, 77555

*Correspondence should be addressed to: Antonella Casola, M.D., Department of Pediatrics, 301 University Blvd., Galveston, TX, 77555-0372; Fax (409) 772-1761; Tel. (409) 747-0581; Email: ancasola@utmb.edu

Running title: RSV and Nrf2

Word count: 5978

References number: 56

Grayscale illustrations: 9

ABSTRACT

Aims: Respiratory syncytial virus (RSV) is the most important cause of viral acute respiratory tract infections and hospitalizations in children, for which no vaccine or treatment is available. RSV infection in cells, mice and children leads to rapid generation of reactive oxygen species, which are associated with oxidative stress and lung damage, due to a significant decrease in the expression of airway antioxidant enzymes (AOEs). Oxidative stress plays an important role of in the pathogenesis of RSV-induced lung disease, as antioxidants ameliorate clinical disease and inflammation *in vivo*. The aim of this study is to investigate the unknown mechanism(s) of viral-induced inhibition of AOE expression. **Results:** This study shows that RSV infection induces a progressive reduction in nuclear and total cellular level of the transcription factor NF-E2-related factor 2 (Nrf2), resulting in decreased binding to endogenous AOE gene promoters and decreased AOE expression. RSV induces Nrf2 deacetylation and degradation via the proteasome pathway *in vitro and in vivo*. Histone deacetylase and proteasome inhibitors block Nrf2 degradation and increase Nrf2 binding to AOE endogenous promoters, resulting in increased AOE expression. Known inducers of Nrf2 are able to increase Nrf2 activation and subsequent AOE expression during RSV infection *in vitro and in vivo*, with significant amelioration of oxidative stress. **Innovation:** This is the first study to investigate the mechanism(s) of viral-induced inhibition of AOE expression. **Conclusion:** RSV-induced inhibition of Nrf2 activation, due to deacetylation and proteasomal degradation, could be targeted for therapeutic intervention aimed to increase antioxidant airway capacity during infection.

INTRODUCTION

Respiratory syncytial virus (RSV) is the single most important virus causing acute respiratory tract infections in children, and is a major cause of severe respiratory morbidity and mortality in the elderly (23), being responsible for 64 million clinical infections and 160 thousand deaths annually worldwide (17). In addition to acute morbidity, RSV infection has been linked to both the development and the severity of asthma. No vaccine or effective treatment is currently available for RSV. In a series of *in vitro* and *in vivo* studies, over the past few years, we have discovered that in the course of RSV infection, reactive oxygen species (ROS) are rapidly generated and they are associated with cellular oxidative damage, indicated by an increase in lipid peroxidation, lung inflammation and clinical disease (10, 24, 25). RSV-induced ROS formation also controls inducible expression of chemokine and other inflammatory genes in response to infection (8, 39). Antioxidant treatment significantly ameliorates RSV-induced clinical disease and pulmonary inflammation in a mouse model of infection, suggesting a casual relationship between increased ROS production and lung disease (10). We found that the expression and activity of the antioxidant enzymes (AOEs) superoxide dismutase (SOD), catalase, glutathione peroxidase (GPx) and glutathione S-transferase (GST) are dramatically decreased in RSV-infected human airway epithelial cells (hAECs)(25). Similar decreases in AOE expression were also observed in the lungs of RSV-infected mice and in nasopharyngeal secretions (NPS) of children with severe RSV-induced lower respiratory tract infection (LRTI)(24), suggesting that oxidative damage associated with RSV infection results from an imbalance between ROS production and antioxidant cellular defenses. Transcription of many oxidative stress-inducible genes is regulated in part through *cis*-acting antioxidant responsive

element (ARE) sequences. This element has been identified in the regulatory regions of genes encoding detoxification enzymes, such as NQO1 (NADPH:quinone oxidoreductase), as well as many AOEs, including SOD1, catalase, heme oxygenase 1, GST and glutathione-generating enzymes such as glutamate cysteine ligase [Reviewed in (32)]. NF-E2-related factor 2 (Nrf2) is an important redox-responsive protein that helps protect the cells from oxidative stress and injury [Reviewed in (29)]. It is a basic leucine zipper transcription factor that is normally bound in the cytosol to a cytoskeleton-associated inhibitor called Keap1 (Kelch-like-ECH associated protein 1) that, when complexed with Nrf2, promotes its ubiquitin-mediated degradation. Electrophile- or ROS-induced release of Nrf2 is proposed to involve covalent modifications of Keap1 and/or Nrf2 in the cytoplasm. Such modifications include oxidation of key cysteine residues in Keap1, phosphorylation of Nrf2, and switching of Cullin-3-dependent ubiquitination from Nrf2 to Keap1, leading to the degradation of Keap1 and stabilization and activation of Nrf2. The released Nrf2 then translocates to the nucleus and binds to ARE sites to promote gene transcription (29). During activation, Nrf2 also undergoes different type of post-translational modifications, including phosphorylation, which regulates nuclear translocation and export (5), as well as acetylation, which is important for stabilization of Nrf2 binding to DNA once activated (33).

The aim of our study was to investigate the unexplored mechanism(s) leading to viral-induced decreased expression of AOE. Our data show that RSV infection induces a progressive reduction in nuclear and total cellular levels of the Nrf2, resulting in decreased binding to ARE site of endogenous AOE gene promoter, with subsequent decrease in their expression. RSV induces Nrf2 deacetylation, ubiquitination, and degradation via the proteasome pathway both *in vitro and in vivo*. Histone deacetylase and proteasome inhibitors block Nrf2 degradation and

increase Nrf2 binding to endogenous promoter ARE sites, resulting in increased AOE expression. Known inducers of Nrf2 are able to increase Nrf2 activation and subsequent AOE expression during RSV infection in airway epithelial cells, as well as in an animal model of infection, with significant amelioration of oxidative stress, which is an important pathogenetic component of viral-induced lung disease, adding additional support to the concept that therapeutic strategies aimed to increase antioxidant airway capacity by increasing Nrf2 activity could be beneficial in RSV infection.

RESULTS

RSV infection downregulates Nrf2-dependent gene transcription. To determine whether Nrf2 activation was affected in response to RSV infection, nuclear proteins isolated from A549 cells infected for various length of time were subjected to Western blot analysis. After an initial modest increase in nuclear translocation, around 6h post-infection (p.i.), there was a progressive, time-dependent decrease in Nrf2 nuclear amounts in infected cells at 15h and later to levels below that of uninfected cells (Figure 1A, left panel). To confirm our findings in A549 cells, a similar experiment was performed in normal human small alveolar epithelial (SAE) cells infected with RSV, in which we observed an identical response, associated with decreased Nrf2 nuclear levels at 15 and 24h p.i. (Figure 1A, right panel). The reduction in nuclear translocation was associated with reduced Nrf2-dependent gene transcription, demonstrated by reporter gene assay. A549 cells were transiently transfected with a synthetic ARE-driven promoter, linked to a luciferase reporter gene, and infected with RSV for 6, 15 and 24h. Nrf2-dependent gene transcription increased at 6h p.i., but then significantly decreased at subsequent time p.i. to values below that of uninfected cells (Figure 1B). To investigate the mechanism, we measured Nrf2 occupancy of the ARE sites of SOD1 and catalase, established Nrf2 target genes whose expression is inhibited by RSV infection, by two-step chromatin immunoprecipitation (XChIP). Nrf2 binding to both promoters was reduced at 15 and 24h p.i., quantitated by genomic PCR (Q-gPCR)(Figure 1C). A similar result was obtained for the NQO1 gene (data not shown).

In a parallel set of experiments, airway epithelial cells were treated with a known pro-oxidative stimulus, hydrogen peroxide, to investigate the effect on Nrf2 activation. Different from what occurs in the context of RSV infection, hydrogen peroxide induced a sustained

increase in Nrf2 nuclear levels, up to 15h post-treatment, investigated by Western blot analysis, with levels returning to basal conditions by 24h (supplementary Figure 1A). The increase in Nrf2 activation was paralleled by an increase in Nfrf2 target genes catalase and SOD1 (supplementary Figure 1B).

RSV infection induces Nrf2 degradation. To determine whether RSV-induced decrease in Nrf2 nuclear levels corresponded to a decrease in total cellular levels, whole cell lysates from A549 and SAE cells infected with RSV for various lengths of time were subjected to Western blot analysis. Both A549 cells (Figure 2A, left panel) and SAE cells (Figure 2A, right panel) showed significantly lower levels of Nrf2 at 15 and 24h p.i., compare to uninfected controls and to early time points of infection, suggesting that RSV induces Nrf2 degradation, possibly through the proteasome pathway. Treatment of A549 cells with the specific proteasome inhibitor lactacystin rescued Nrf2 cellular levels (Figure 2B), indicating that Nrf2 degradation associated with RSV infection occurs through the proteasome. To investigate whether RSV induced changes in Nrf2 ubiquitination, total cell lysate of airway epithelial cells infected with RSV for 18h in the presence or absence of lactacystin (10 μM) were immunoprecipitated with anti-Nrf2 antibody and subjected to Western blot analysis using an anti-ubiquitin antibody. RSV infection was associated with increased Nrf2 ubiquitination, compared to uninfected cells (Figure 2C), suggesting that this is an important mechanism(s) targeting Nrf2 to proteasome degradation. Similar results were observed in RSV-infected SAE cells (data not shown).

Treatment of airway epithelial cells with proteasome inhibitors led not only to increased Nrf2 cellular levels, but also rescued Nrf2 function, as MG132, another proteasome inhibitor,

and lactacystin treatment was associated with increased ARE-dependent gene transcription, shown by reporter gene assays (Figure 3A) and AOE gene expression, quantitated by Q-RT-PCR (Figure 3B), as well as increased Nrf2 binding to the endogenous SOD1 and catalase ARE sites, assessed by XChIP (Figure 3C). From these data, we conclude that proteasome inhibition can restore Nrf2 expression and function in the context of RSV infection.

RSV infection is associated with Nrf2 deacetylation. Acetylation is a post-translational modification important for stabilization of Nrf2 binding to DNA once activated (33). To determine whether RSV infection could modulate Nrf2 acetylation, total cell lysates from A549 cells were immunoprecipitated with anti-Nrf2 antibody and subjected to Western blot using anti acetyl-lysine antibody. RSV infection was associated with a significant decrease in basal Nrf2 acetylation, both in A549 (Figure 4A, left panel), as well as in SAE cells (Figure 4A, right panel), starting as early as 6h p.i. (data shown represent 15 h p.i.). Treatment of airway epithelial cell with the histone deacetylase (HDAC) inhibitor Trichostatin A (TSA) significantly restored Nrf2 acetylation, leading to some increase in Nrf2 cellular levels (Figure 4A, input). RSV infection upregulated nuclear HDAC activity, starting at 6h p.i. and continuing up to 24h p.i., both in A549 (Figure 4B, left panel), as well as in SAE cells (Figure 4B, right panel). In addition, RSV infection was associated with a significant reduction of binding of the transacetylase CBP to the ARE site of the SOD1 gene promoter, starting around 15h p.i., after an initial increase in binding at early time points of infection, as determined by XChIP assay (Figure 4C). Increasing CBP expression by transient transfection was able to rescue ARE-driven reporter gene activity in

viral-infected cells (Figure 4D), supporting the idea that Nrf2 deacetylation could be the result of unbalanced HDAC and acetylation activity.

Inhibition of HDAC activity was able to rescue nuclear levels of Nrf2 during viral infection, as shown by Western blot analysis of nuclear fractions from A549 cells (Figure 5A, left panel) and SAE cells (Figure 5A, right panel), and, importantly, it was also associated with an overall increase in Nrf2 cellular levels, assessed by Western blot analysis of total cell lysates from A549 cells (Figure 5B, left panel) and SAE cells (Figure 5B, right panel).

Inhibition of HDAC activity was also able to restore ARE-dependent gene transcription, as shown by reporter gene assay in A549 cells transiently transfected with the ARE-driven promoter and infected with RSV in the presence or absence of TSA (Figure 5C), leading to increased expression of Nrf2 target genes, such as SOD1 and catalase, assessed by q-RT-PCR, both in A549 (Figure 5D, upper panel) and SAE cells (Figure 5D, lower panel). Increased AOE expression was associated with a significant increase of Nrf2 occupancy of the catalase and SOD1 promoter ARE sites (Figure 5E), supporting the finding that inhibition of HDAC can rescue Nrf2 activation in the context of RSV infection.

HDAC 1 and 2 play an important role in RSV-induced inhibition of Nrf2 activation. Human HDACs are classified, based on the sequence similarity and cofactor dependency, into three groups (22). TSA is broad specific inhibitor and it blocks both Class I & II HDAC activity (15). As shown before, TSA treatment in airway epithelial cells infected with RSV infection was able to rescue Nrf2 activation. On the other hand, the HDAC class III specific inhibitor Ex-527 (18) did not have a significant effect, indicating that these class of HDAC proteins was not involved

in RSV-induced Nrf2 inhibition (data not shown). Since HDAC class II proteins are present predominantly in skeletal muscle, heart, brain, and thymus (54, 55), we first investigated the role of HDAC class I proteins, specifically HDAC1, 2 and 3, in RSV-induced Nrf2 deacetylation, as they are known to modulate activation of other transcription factors such as Nuclear Factor (NF)-κB and Signal Transducer and Activator of Transcription (STAT)(36, 51). We first determined whether there was any change in HDAC expression. A549 cells were infected with RSV, harvested at different time points after infection to prepare nuclear proteins, and HDAC 1, 2 and 3 levels were assessed by Western blot analysis. There was no difference in nuclear levels of any of the three HDAC proteins (supplementary Figure 2), indicating that change in total HDAC activity was not due to their increased expression. We then inhibited their expression using specific siRNAs. A549 were transfected with either scrambled or siRNAs selectively targeting HDAC1, 2 or 3, infected with RSV, and harvested to prepare either nuclear extracts or total RNA. Western blots analysis showed that Nrf2 nuclear levels in HDAC1 and 2 siRNA transfected cells were significantly higher compared to those of scramble transfected ones, following infection with RSV, with HDAC1 siRNA being the most effective in restoring Nrf2 activation to levels comparable of that of uninfected cells (Figure 6A and B), while there was no significant change observed in HDAC3 siRNA transfected cells (Figure 6C). In agreement with these findings, mRNA levels of the Nrf2 target genes catalase and SOD1 were significantly higher in RSV-infected cells transfected with siRNA for HDAC1 and 2, but not HDAC3, compared to scrambled (Figure 6D).

To determine whether HDAC1 was binding to the ARE site of the SOD1 gene promoter, we performed XChIP/Q-gPCR. HDAC1 occupancy of the SOD1 ARE site was significantly

lower in RSV-infected cells at 6h p.i., below levels of uninfected cells, however it increased significantly at 15h p.i. (Figure 6E). Treatment of infected cells with TSA resulted in a significant inhibition of HDAC1 recruitment to the SOD1 ARE site (Figure 6E), in agreement with the previously observed changes in Nrf2 activation.

Nrf2 is deacetylated and degraded through the proteasome i*n vivo*. To determine whether deacetylation and proteasome degradation played a role in viral-induced inhibition of Nrf2 activation *in vivo*, we performed confirmatory experiments in our mouse model of RSV infection. Nuclear proteins isolated from lungs of mice either sham-inoculated or infected with RSV for 48h were tested for HDAC activity and Nrf2 acetylation, as described in the *in vitro* experiments. Similar to our findings in airway epithelial cells, RSV infection was associated with increased HDAC activity (Figure 7A), as well as a significant decrease in basal Nrf2 acetylation, along with reduced Nrf2 nuclear levels (Figure 7B).

To determine whether inhibition of proteasome activity could rescue Nrf2 expression and ARE-dependent gene expression, mice were treated with MG132 one hour prior to viral infection and harvested to prepare nuclear extract or extract total RNA at 48h p.i. Mice infected with RSV and treated with MG132 showed significantly increased Nrf2 nuclear levels, compared to untreated infected mice (Figure 7C). Proteasome inhibition was also able to significantly increase SOD1 expression during RSV infection, while there was only a modest rescue of catalase expression (Figure 7D).

Nrf2 inducers ameliorate oxidative stress during RSV infection *in vitro* and *in vivo*. Among the compounds known to stimulate ARE-driven transcription (26), butylated hydroxynanisol (BHA) and its metabolite *tert*-butylhydroquinone (tBHQ) have been shown to increase HO-1, NQO1 and Nrf2 protein expression in both primary and cultured cells (35). Since BHA was effective in decreasing RSV-induced oxidative stress (25), we investigated whether tBHQ treatment could rescue Nrf2 activity following viral infection (35). A549 cells were transiently transfected with the ARE-driven reporter plasmid and infected with RSV in the presence or absence of tBHQ. RSV infection was associated with a significant decrease in reporter gene activity, compared to uninfected cells, which was restored close to levels of uninfected cells by tBHQ treatment (Figure 8A). AOE gene and protein expression, as well as Nrf2 nuclear levels, were also significantly increased in RSV-infected cells by tBHQ treatment (Figure 8B and C), indicating that Nrf2 inducers can restore ARE-dependent gene expression following RSV infection. Treatment of airway epithelial cells with tBHQ up to 6h p.i. was able to restore Nrf2 activation and ARE-dependent gene expression in response to RSV infection (supplementary Figure 3), but not at later time points of infection (data not shown). Restoration of AOE cellular capacity was paralleled by a significant reduction of RSV-induced oxidative stress, as shown by a significant decrease of the oxidative marker 8-isoprostane in viral-infected, tBHQ-treated cells (Figure 8D). The effect of tBHQ treatment on Nrf2 activation was not due to changes in HDAC activity (Figure 8E).

As tBHQ treatment of airway epithelial cells was able to rescue Nrf2 activation, we tested whether BHA (precursor of tBHQ) had a similar effect in the airways of infected mice. Lungs of mice either sham-inoculated or infected with RSV for 48h in the presence or absence of

BHA (250 mg/kg) were harvested to prepare bronchoalveolar lavages (BALs), nuclear extracts or total RNA. Mice infected with RSV showed significantly reduced Nrf2 nuclear levels, compared to sham-inoculated mice, and, in most of the infected mice, BHA treatment was able to restore Nrf2 activation to levels close to that of uninfected mice (Figure 9A), as well as the expression of the Nrf2 target genes catalase and SOD1 (Figure 9B). In addition, there was a very significant reduction in RSV-induced lung oxidative stress in BHA-treated mice, as indicated by a significant reduction of BAL 8-isoprostane levels in BALs, compared to untreated, infected mice (Figure 9C), supporting our previous findings that BHA treatment has a positive impact on RSV-induced lung disease.

DISCUSSION

Since its isolation, RSV has been identified as a leading cause of epidemic LRTIs in infants and children worldwide (23). No efficacious treatment or vaccine yet exists for RSV and immunity is incomplete, resulting in repeated attacks of acute respiratory tract illness through adulthood (23). Several recent studies have directly or indirectly indicated an important role of ROS produced by epithelial and inflammatory cells, and subsequent oxidative stress, in the pathogenesis of acute and chronic lung inflammatory diseases such as acute respiratory distress, cystic fibrosis, asthma and COPD (40, 42, 44, 47). We and others have shown that infection with RSV, the recently identified human metapneumovirus (hMPV), and influenza can all induce ROS formation (4, 8, 12, 28, 30) and that inhibiting ROS production by administering antioxidants or recombinant SODs significantly decreases lung injury and improves clinical disease in RSV- and influenza-infected animals, suggesting that ROS play a significant role in the pathogenesis of virus-induced pneumonia (1, 2). Although increased antioxidant defenses have been reported in certain pulmonary diseases resulting from exposure to hyperoxia (16), ozone (6) and cigarette smoke (19), our recent studies show that RSV infection induces a significant decrease in the expression of most AOEs involved in maintaining the cellular oxidant-antioxidant balance, leading to cellular oxidative stress, both *in vitro* and *in vivo* .

AOE gene transcription is regulated through binding of Nrf2 to the ARE site located in the gene promoters (29). Several viruses have been shown to induce ARE-dependent responses by activating Nrf2. Among them, hepatitis B and C viruses, human cytomegalovirus and the Kaposi's sarcoma-associated herpes virus, which can all induce ROS formation [Reviewed in (12)], have been shown to activate Nrf2 in infected cells, leading to the induction of

cytoprotective genes, as a mechanism to protect infected cells from oxidative damage (7, 21, 27, 38, 48). Similarly, Marburg virus, an important cause of human hemorrhagic fever, blocks Keap1 activation, leading to the expression of AOE genes, to ensure survival of infected cells (45). In our study, we found that RSV infection of airway epithelial cells induces a transient Nrf2 activation, demonstrated by increased Nrf2 binding to the ARE of the AOE gene promoter and activation of ARE-dependent gene transcription at 6h p.i., followed however by a progressive decrease in Nrf2 activation, starting at 15h p.i., to levels below the ones found in uninfected cells (Figure 1), with a kinetics that mirror the progressive decrease in AOE expression observed in RSV-infected cells (25).

Reduced nuclear levels of Nrf2 can occur as a result of various mechanisms, including decreased expression, increased degradation or through increased nuclear export (32). Our results show that RSV infection is associated with increased Nrf2 ubiquitination and degradation through a proteasomal pathway, based on our observations that the proteasomal inhibitors MG132 and Lactacystin rescue Nrf2 expression and binding to the ARE site of the AOE gene promoters, restoring ARE-dependent gene transcription and AOE gene expression to that of uninfected cells (Figure 2 and 3). Nrf2 degradation through the proteasome pathway occurred also *in vivo*, as MG132 treatment in mice was able to restore Nrf2 nuclear levels in lungs of mice infected with RSV, however it had a modest impact on rescuing AOE gene expression, in particular on catalase (Figure 7). A possible explanation of these findings is that MG132 affects activation of other signaling molecules which in turn could be important in regulating AOE gene expression. For example, MG132 inhibits NF-κB activation (31), and NF-κB seems to play an important role in transcriptional response to oxidative stress, including the expression of catalase

and glutathione peroxidase (56). Although stabilization of Nrf2 by proteasome inhibition and subsequent transcriptional activation of its downstream genes, by preventing Nrf2 degradation, have been shown in different cell types and disease conditions [Reviewed in (13)], suggesting that proteasome inhibition could be a promising therapeutic strategy for oxidative stress damage-associated diseases, it does not seem to have a beneficial effect in the context of RSV, at least in a mouse model of infection (41). Treatment of RSV infected mice with bortezomib, an FDA approved proteasome inhibitor, resulted in increased pulmonary inflammation and disease, compared to untreated, infected animals. Whether Nrf2 ubiquitination in response to RSV infection occurs through Keap1, it remains to be established, as we observed it both in SAE and A549 cells, which carries a Keap1 mutation that greatly reduces its repressor activity (50).

RSV-induced decrease in Nrf2 activation could be rescued by treatment of airway epithelial cells with the Nrf2 inducer tBHQ, shown by restoration of Nrf2 nuclear levels, ARE-dependent gene transcription and AOE expression, which resulted in a significant decrease of cellular oxidative stress (Figure 8). Administration of tBHQ was also able to rescue Nrf2 activation *in vivo*, as indicated by a significant increase of Nrf2 nuclear levels in lung extracts of RSV-infected mice, which were dramatically decreased by the infection (Figure 9), as we have previously described (24). The Nrf2-ARE pathway has been shown to play a protective role in the murine airways against RSV-induced injury and oxidative stress. More severe RSV disease, including higher viral titers, augmented inflammation, and enhanced mucus production and epithelial injury were found in *Nrf2-/-* mice compared to *Nrf2+/+* mice (11). Similarly, lack of Nrf2 expression resulted in increased influenza virus replication (34), while treatment of airway

epithelial cells with the Nrf2 inducer sulforaphane or Nrf2 overexpression led to significant inhibition of viral replication and oxidative stress (34, 37).

Post-translational modifications, such as phosphorylation and acetylation, are important regulators of transcription factor activation, regulating multiple steps of activation, from nuclear translocation, to DNA-binding to transcriptional activity. Nrf2 has been shown to be acetylated by p300/CBP (52). Acetylation promotes DNA binding of Nrf2 and enhances gene transcription, although not of all Nrf2 target genes (52). It also regulates Nrf2 cellular distribution, as deacetylating conditions results in relocalization of Nrf2 to the cytoplasmic compartment (33). As a dynamic and reversible process, acetylation of Nrf2 is determined by the relative activities of HATs and histone deacetylases. Our results show that RSV infection was associated with increased deacetylase activity and reduced recruitment of CBP to the ARE site of AOE gene promoters, resulting in Nrf2 deacetylation both *in vitro* and *in vivo* (Figure 4 and 7). CBP overexpression could rescue ARE-dependent gene transcription and treatment of infected cells with the HDAC inhibitor TSA led to restoration of Nrf2 acetylation, suggesting that RSV infection is associated with an unbalance acetylation/deacetylation environment at the ARE transcription sites. HDAC inhibition was able to restore Nrf2 nuclear levels and Nrf2 binding to the ARE site of AOE gene promoters, therefore restoring ARE-dependent gene transcription and gene expression in RSV-infected cells (Figure 5). Importantly, HDAC inhibition was also associated with increased Nrf2 cellular levels (Figure 5), suggesting that blocking RSV-induced Nrf2 deacetylation might indeed protect Nrf2 against degradation by retaining it in the nucleus, bound to its cognate promoter site. Although HDAC class III (sirtuins) have been shown to play a role in Nrf2 deacetylation (33), we could not demonstrate a significant role of this class of

HDAC in RSV-induced inhibition of Nrf2 activation. On the other hand, class I HDAC1 and 2 seem to be important in regulating Nrf2 function in infected cells, as inhibition of their expression was associated with restoration of Nrf2 nuclear levels and Nrf2-dependent gene expression both in A549 and SAE cells (Figure 6). Although we did observe an increase in HDAC activity, there was no induction of HDAC 1 or 2 expression in RSV-infected cells (Supplementary Figure 2). Induction of global HDAC activity has been reported in other disease models, such as cardiac hypertrophy and ischemia-reperfusion injury, as well as rheumathoid arthritis (20, 43). HDAC1 and 2 activity is regulated at multiple levels [reviewed in (14)]. Both proteins are active within a complex of proteins, the better characterized being Sin3, NuRD (nucleosome remodelling and deacetylating) and Co-REST, which are necessary for modulating HDAC deacetylase activity and DNA-binding, together with other proteins that mediate the recruitment of HDACs to gene promoters. A second way of regulating HDAC activity is via post-translational modifications. Both activity and complex-formation are regulated by phosphorylation. HDAC1 and HDAC2 are phosphorylated at a low level in resting cells and hyperphosphorylation leads to a significant increase in deacetylase activity. It is possible that RSV infection leads to modification of either or both of these important regulatory elements of HDAC activation. HDAC inhibitors are currently being developed as a new class of anti-cancer agents, many of which have already entered clinical trials, and our findings suggest that they could represent an attractive novel treatment for viral-induced lung inflammation.

In conclusion, RSV-induced respiratory disease is associated with increased ROS generation and oxidative stress that are likely to play a key role in initiating and amplifying lung injury and inflammation. Compounds that stimulate ARE-driven transcription, as well as

possibly HDAC inhibitors, could hold great potential for modulating RSV-induced oxidative stress and the associated lung damage.

INNOVATION

The innovative aspects of this study lies in the identification of a mechanism responsible for decrease activation of Nrf2, a key regulator of airway antioxidant defenses, which likely play an important role in lung injury due to respiratory viral infections. Although excessive ROS formation usually induces adaptive responses that upregulate the antioxidant defense networks, RSV infection interferes with this response, resulting in inhibition of several key antioxidant and cytoprotective enzymes, due to a defect in Nrf2 activation. Treatment directed to restore Nrf2 activation and subsequent antioxidant enzyme machinery could represent a novel therapeutic approach for virus-mediated airway disease.

MATERIALS AND METHODS

Materials. BHA, tBHQ and TSA were purchased from Sigma., MO, USA. MG132 and Lactacystin were purchased from Calbiochem, CA, USA.

RSV preparation. The RSV Long strain was grown in Hep-2 cells and purified by centrifugation on discontinuous sucrose gradients as described elsewhere (53). The virus titer of the purified RSV pools was 8-9 $\log_{10}$ plaque forming units (PFU)/mL using a methylcellulose plaque assay. No contaminating cytokines were found in these sucrose-purified viral preparations (46). LPS, assayed using the limulus hemocyanin agglutination assay, was not detected. Virus pools were aliquoted, quick-frozen on dry ice/alcohol and stored at -70 ^{o}C until used.

Cell Culture and Infection of Epithelial Cells with RSV. A549 cells, a human alveolar type II like epithelial cell line (American Type Culture Collection, Manassas, VA) and small alveolar epithelial (SAE) cells (from Clonetics, now part of Lonza Inc., San Diego, CA), normal human airway epithelial cells derived from terminal bronchioli, were grown according to the manufacturer's instructions. A549 cells were maintained in F12K medium containing 10% (vol/vol) FBS, 10 mM glutamine, 100 IU/ml penicillin, and 100 μg/ml streptomycin. SAE cells were maintained in small airway epithelial cell (SAEC) growth medium containing 7.5 mg/ml bovine pituitary extract (BPE), 0.5 mg/ml hydrocortisone, 0.5 μg/ml hEGF, 0.5 mg/ml epinephrine, 10 mg/ml transferrin, 5 mg/ml insulin, 0.1 μg/ml retinoic acid, 0.5 μg/ml triiodothyronine, 50 mg/ml gentamicin, and 50 mg/ml bovine serum albumin (BSA). RSV infection in A549 cells were done in F12K medium containing 2% FBS. When SAE were used

for RSV infection, they were changed to basal medium, not supplemented with growth factors, 6 hours before and throughout the length of the experiment. At around 80 to 90% confluence, cell monolayers were infected with RSV at multiplicity of infection (MOI) of 3. An equivalent amount of a 30% sucrose solution was added to uninfected A549 and SAE cells, as a control.

For tBHQ and TSA experiments, cells were pretreated with the compounds for 1 hour and then infected in their presence for the duration of the experiment. In selected experiments, tBHQ was also added at different time points after infection. For proteasome inhibitors experiments, MG132 or Lactacystin were added 10h post-infection. Equal amounts of diluent were added to cells uninfected and infected as control. Total number of cells and cell viability, following various treatments, were measured by trypan blue exclusion. There was no significant change in cell viability with all compounds tested. Similarly, there was no effect of both compounds on viral replication, tested by plaque assay.

Reporter gene assay. Logarithmically growing A549 cells were transfected in triplicate in 24 well plates dishes with Cignal Antioxidant Response Reporter from Qiagen, (Cat # 336841, Maryland) an optimized luciferase reporter construct that monitors both increases and decreases in the transcriptional activity of Nrf2, using Fugene 6 (Cat # E2692, Promega Corp, Madison, WI) . Briefly, 0.5 μg of the reporter gene plasmid and 0.05 μg of β-galactosidase expression plasmid/well were premixed with FuGene 6 and added to the cells in one ml of regular medium. The next morning, cells were infected with RSV in the presence or absence of specific inhibitors and harvested at 24 h p.i. to independently measure luciferase and β-galactosidase reporter activity, as previously described (9). Luciferase activity was normalized to the internal control

β-galactosidase activity. Results are expressed in arbitrary units. All experiments were performed an average of three times.

Western blot. Nuclear extracts of uninfected and infected cells were prepared using hypotonic/nonionic detergent lysis, according to Schaffner protocol (49). To prevent contamination with cytoplasmic proteins, isolated nuclei were purified by centrifugation through 1.7 M sucrose buffer A for 30 minutes, at 12,000 rpm, before nuclear protein extraction, as previously described (3, 49). Total cell lysates of uninfected and infected cells were prepared by adding ice-cold lysis buffer (50mM Tric-HCl, pH 7.4, 150mM NaCl, 1mM EGTA, 0.25% sodium deoxycholate, 1mM Na_3VO_4, 1mM NaF, 1% Triton X-100 and 1 μg/ml of aprotinin, leupeptin and pepstatin). After incubation on ice for 10 min, the lysates were collected and detergent insoluble materials were removed by centrifugation at 4^{o}C at 14,000 g. After normalizing for protein content, using Bio-Rad, Hercules, CA, equal amount of proteins (10 to 20 μg) were loaded and separated by 8 % SDS-PAGE, and transferred onto polyvinylidene difluoride Immobilon-P membrane (IPVH00010, Millipore CA, USA). Nonspecific binding was blocked by immersing the membrane in Tris-buffered saline-Tween (TBST) blocking solution (10 mM Tris-HCl, pH 7.6, 150 mM NaCl, 0.05% Tween-20 [v/v]) containing 5% skim milk powder for 30 minutes at room temperature. After a short wash in TBST, the membranes were incubated with the primary antibody overnight at 4°C, followed by the appropriate secondary antibody (Santa Cruz Biotechnology, Santa Cruz, CA), diluted 1:10,000 in TBST for 1 hour at room temperature. After washing, the proteins were detected using enhanced-chemiluminescence assay (RPN 2016, Amersham, GE Healthcare, UK) according to the manufacturer's

recommendations. Densitometric analysis of band intensities was performed using UVP VisionWorksLS Image Aquasition and Analysis Software 8.0 RC 1.2 (UVP, Upland, CA) . The primary antibodies used for Western blots were anti-Nrf2 (H-300, sc-13032), anti HDAC1(H-51, sc-7872), -HDAC2 (H-54, sc-7899), -HDAC3 (H-99, sc-11417) from Santa Cruz Biotechnology Inc, CA, anti-SOD1 (SOD100, Stressgen Bioreagents, MI), anti-lamin B (GWB5CD4D4, GenWay Biotech) and anti-β-Actin (A1978 Sigma, MO).

Immunoprecipitation. 250µg of total cell lysate or 200 µg of nuclear extracts from RSV-infected A549 or SAE cells were immunoprecipitated using 5µg of anti-Nrf2 antibody and protein A/G agarose beads (Santa Cruz Biotechnology Inc, sc-2003). Complexes were eluted in 2x SDS PAGE buffer and subjected to Western blot analysis using anti-ubiquitin (SC-8017, Santa Cruz Biotechnology Inc, CA) or anti-acetyl lysine (ab21623, Abcam, MA) antibodies.

HDAC Activity. Nuclear extracts prepared from A549 cells and SAE cells uninfected or infected with RSV were assayed for HDAC activity using a commercially available kit (10011563, Cayman, Ann Arbor, MI,), according to the manufacturer's instructions.

8-Isoprostane assay. Measurements of F_2 8-isoprostane was performed using a competitive enzyme immunoassay from Cayman Chemical (Cat 516351, Ann Arbor, MI).

Quantitative Real Time PCR (Q-RT-PCR). Total RNA was extracted using ToTALLY RNA kit from Ambion (Cat # AM1910, Austin, TX)). RNA samples were quantified using a Nanodrop

Spectrophotometer (Nanodrop Technologies) and quality was analyzed on RNA Nano or Pico chip using the Agilent 2100 Bioanalyzer (Agilent Technologies, Santa Clara, CA. Synthesis of cDNA was performed with 1ug of total RNA in a 20ul reaction using the reagents in the Taqman Reverse Transcription Reagents Kit from ABI (Applied Biosystems #N8080234). The reaction conditions were as follows: 25ºC, 10 minutes, 48ºC, 30 minutes, 95ºC, 5 minutes. Q-PCR amplifications (performed in triplicate) was done using 1µl of cDNA in a total volume of 25µl using the Faststart Universal SYBR green Master Mix (Roche Applied Science #04913850001). The final concentration of the primers was 300nM. 18S RNA was used as housekeeping gene for normalization. PCR assays were run in the ABI Prism 7500 Sequence Detection System with the following conditions: 50ºC, 2 minutes, 95ºC, 10 minutes and then 95ºC, 15 seconds, 60ºC, 1 minute for forty cycles. Duplicate CT values were analyzed in Microsoft Excel using the comparative CT (ΔΔCT) method as described by the manufacturer (Applied Biosystems). The amount of target ($2^{-\Delta\Delta CT}$) was obtained by normalizing to endogenous reference (18S) sample.

Two-step Chromatin immunoprecipitation (XChIP) and quantitative genomic (Q-gPCR). For XChIP we used ChIP-IT Express kit from Active Motif (Cat # 53008 & 53032, Carlsbad, CA) and followed manufacturer instruction with slight modification. Briefly, A549 cells in 10 cm plate were washed three times with PBS and fixed with freshly prepared 2mM disuccinimidyl gluterate (DSG) (Cat # 20593, Thermo Scientific, Rockford, IL). After three washes with PBS, cells were fixed with freshly prepared formaldehyde for 1 min and neutralized with glycine for 5 min at room temperature. Cells were harvested and disrupted using a dounce homogenizer to isolate nuclei. Nuclei were sheared by sonication to obtain DNA fragments from 200 to 1500

base pair (bp). 20 micrograms of sheared chromatin were immunoprecipitated with 5 µg of ChIP grade anti-Nrf 2 (sc-722X), -CBP (sc-369X), -or HDAC1 (sc-7872X) antibody from Santa Cruz Biotechnology, CA, USA, and magnetic beads conjugated with protein G at 4ºC overnight. Immunoprecipitation with IgG antibody was used as negative control. Chromatin was reverse crosslinked, eluted from magnetic beads, and purified using PCR purification kit (Cat # 28106, Qiagen GmbH, Hilden). Q-gPCR was done by SyBR green based real time PCR using the following primers spanning the SOD1 gene promoter ARE site: forward-AAAGCATCCATCTTGGGGCG and reverse- AACCTTCTTTTCACGGGGGC, or the catalase promoter ARE site: forward-AACGGCCGCGTCCCAG and reverse-CTCTCCGAAGGAGGCCTGAA. Total input chromatin DNA for immunoprecipitation was included as positive control for PCR amplification.

In vivo studies. 12 weeks old female BALB/c mice were purchased from Harlan (Houston, TX) and were housed in pathogen-free conditions in the animal research facility of the University Texas Medical Branch (UTMB), Galveston, Texas, in accordance with the National Institutes of Health and UTMB institutional guidelines for animal care. Under light anesthesia, mice were inoculated intranasally with 10^7 PFU of sucrose-purified RSV (Long Strain) in a final volume of 50 µl/dose diluted in phosphate buffered saline (PBS). Control animals (mock infected, defined as sham) received PBS treated in a similar manner. Mice were treated by gavage with 250mg/kg body weight of BHA or corn oil (diluents for BHA) 2 days prior RSV infection and during the first 2 days of infection. Bronchoalveolar lavages were prepared by flushing the lungs twice via the trachea with 1 mL of ice-cold PBS. BAL fluid supernatant were collected at 48 hours post-

infection following centrifugation (5 min at 5000 rpm), and stored at -80°C prior to 8-isoprostane assay. Lungs samples from all groups were harvested at 48 hours p.i. to assess mRNA levels of SOD1 and catalase by Q-RT-PCR, and Nrf2 nuclear levels by Western blot. Mice were given i.n. proteasome inhibitor MG-132 (Calbiochem, Massachusetts) at 10μg/dose, or an appropriate volume of vehicle, 1 hour before infection. Lungs samples from all groups were harvested at 48 hours p.i. to assess mRNA levels of SOD1 and catalase by Q-RT-PCR, and Nrf2 nuclear levels by Western blot.

Statistical analysis. All results are expressed as mean ± SEM. Data were analyzed using the GraphPad Prism 5 software. Results were compared among treatment groups by one-way ANOVA, assuming a type I error of 0.05. Significant differences between treatments were identified by the Tukey's post-hoc test. Significance was accepted at $p<0.05$. To streamline figures, all significant results were reported as $p<0.05$, although in many instances it was well below that threshold.

ACKNOWLEDGMENTS

This project was supported by W81XWH1010146-DoD. We would like to acknowledge Tianshuang Liu and Yinghong Ma for their technical assistance, and Cynthia Tribble for manuscript editing and submission.

LIST OF ABBREVIATIONS

AOE	Antioxidant enzyme
ARE	Antioxidant response element
BHA	Butylated hydroxyanisole
ChIP	Chromatin immunoprecipitation
HDAC	Histone deacetylase
IP	Immunoprecipitation
Keap1	Kelch like-ECH-associated protein 1
Nrf2	Nuclear factor erythroid 2–related factor 2
QgPCR	Quantitative genomic PCR
ROS	Reactive oxygen species
RSV	Respiratory syncytial virus
SAE	Small Airway Epithelial Cells
SOD1	Superoxide dismutase 1
tBHQ	t-Butylhydroquinone
TSA	Trichostatin A
Ub	Ubiquitin

REFERENCES

1. Akaike T, Ando M, Oda T, Doi T, Ljiri S, Araki S et al. Dependence on O2 generation by xanthine oxidase of pathogenesis of influenza virus infection in mice. *J Clin Invest* 85, 1990.
2. Akaike T, Noguchi Y, Ijiri S, Setoguchi K, Suga M, Zheng YM et al. Pathogenesis of influenza virus-induced pneumonia: involvement of both nitric oxide and oxygen radicals. *Proc Natl Acad Sci U S A* 93: 2448-2453, 1996.
3. Bao X, Liu T, Shan Y, Li K, Garofalo RP, Casola A. Human metapneumovirus glycoprotein G inhibits innate immune responses. *PLoS Pathog* 4: e1000077, 2008.
4. Bao X, Sinha M, Liu T, Hong C, Luxon BA, Garofalo RP et al. Identification of human metapneumovirus-induced gene networks in airway epithelial cells by microarray analysis. *Virology* 374: 114-127, 2008.
5. Bloom DA, Jaiswal AK. Phosphorylation of Nrf2 at Ser40 by protein kinase C in response to antioxidants leads to the release of Nrf2 from INrf2, but is not required for Nrf2 stabilization/accumulation in the nucleus and transcriptional activation of antioxidant response element-mediated NAD(P)H:quinone oxidoreductase-1 gene expression. *J Biol Chem* 278: 44675-44682, 2003.
6. Boehme DS, Hotchkiss JA, Henderson RF. Glutathione and GSH-dependent enzymes in bronchoalveolar lavage fluid cells in response to ozone. *Exp Mol Pathol* 56: 37-48, 1992.
7. Burdette D, Olivarez M, Waris G. Activation of transcription factor Nrf2 by hepatitis C virus induces the cell-survival pathway. *J Gen Virol* 91: 681-690, 2010.

8. Casola A, Burger N, Liu T, Jamaluddin M, Brasier A.R., Garofalo RP. Oxidant tone regulates RANTES gene transcription in airway epithelial cells infected with Respiratory Syncytial Virus: role in viral-induced Interferon Regulatory Factor activation. *J Biol Chem* 276: 19715-19722, 2001.
9. Casola A, Garofalo RP, Jamaluddin M, Vlahopoulos S, Brasier AR. Requirement of a novel upstream response element in RSV induction of interleukin-8 gene expression: stimulus-specific differences with cytokine activation. *J Immunol* 164: 5944-5951, 2000.
10. Castro SM, Guerrero-Plata A, Suarez-Real G, Adegboyega PA, Colasurdo GN, Khan AM et al. Antioxidant Treatment Ameliorates Respiratory Syncytial Virus-induced Disease and Lung Inflammation. *Am J Respir Crit Care Med* 174: 1361-1369, 2006.
11. Cho HY, Imani F, Miller-Degraff L, Walters D, Melendi GA, Yamamoto M et al. Antiviral Activity of Nrf2 in a Murine Model of Respiratory Syncytial Virus (RSV) Disease. *Am J Respir Crit Care Med* 179:138-50, 2008.
12. Choi AM, Knobil K, Otterbein SL, Eastman DA, Jacoby DB. Oxidant stress responses in influenza virus pneumonia: gene expression and transcription factor activation. *Am J Physiol* 271: L383-L391, 1996.
13. Cui W, Bai Y, Luo P, Miao L, Cai L. Preventive and therapeutic effects of MG132 by activating Nrf2-ARE signaling pathway on oxidative stress-induced cardiovascular and renal injury. *Oxid Med Cell Longev* 2013: 306073, 2013.
14. de Ruijter AJ, van Gennip AH, Caron HN, Kemp S, van Kuilenburg AB. Histone deacetylases (HDACs): characterization of the classical HDAC family. *Biochem J* 370: 737-749, 2003.

15. Dokmanovic M, Clarke C, Marks PA. Histone deacetylase inhibitors: overview and perspectives. *Mol Cancer Res* 5: 981-989, 2007.
16. Erzurum SC, Danel C, Gillissen A, Chu CS, Trapnell BC, Crystal RG. In vivo antioxidant gene expression in human airway epithelium of normal individuals exposed to 100% O2. *J Appl Physiol* 75: 1256-1262, 1993.
17. Falsey AR, Hennessey PA, Formica MA, Cox C, Walsh EE. Respiratory syncytial virus infection in elderly and high-risk adults. *N Engl J Med* 352: 1749-1759, 2005.
18. Gertz M, Fischer F, Nguyen GT, Lakshminarasimhan M, Schutkowski M, Weyand M et al. Ex-527 inhibits Sirtuins by exploiting their unique NAD+-dependent deacetylation mechanism. *Proc Natl Acad Sci U S A* 110: E2772-E2781, 2013.
19. Gilks CB, Price K, Wright JL, Churg A. Antioxidant gene expression in rat lung after exposure to cigarette smoke. *Am J Pathol* 152: 269-278, 1998.
20. Gillespie J, Savic S, Wong C, Hempshall A, Inman M, Emery P et al. Histone deacetylases are dysregulated in rheumatoid arthritis and a novel histone deacetylase 3-selective inhibitor reduces interleukin-6 production by peripheral blood mononuclear cells from rheumatoid arthritis patients. *Arthritis Rheum* 64: 418-422, 2012.
21. Gjyshi O, Bottero V, Veettil MV, Dutta S, Singh VV, Chikoti L et al. Kaposi's sarcoma-associated herpesvirus induces Nrf2 during de novo infection of endothelial cells to create a microenvironment conducive to infection. *PLoS Pathog* 10: e1004460, 2014.
22. Gregoretti IV, Lee YM, Goodson HV. Molecular evolution of the histone deacetylase family: functional implications of phylogenetic analysis. *J Mol Biol* 338: 17-31, 2004.

23. Hall CB. Respiratory syncytial virus and parainfluenza virus. *N Engl J Med* 344: 1917-1928, 2001.

24. Hosakote YM, Jantzi PD, Esham DL, Spratt H, Kurosky A, Casola A et al. Viral-mediated inhibition of antioxidant enzymes contributes to the pathogenesis of severe respiratory syncytial virus bronchiolitis. *Am J Respir Crit Care Med* 183:1550-1560, 2011.

25. Hosakote YM, Liu T, Castro SM, Garofalo RP, Casola A. Respiratory syncytial virus induces oxidative stress by modulating antioxidant enzymes. *Am J Respir Cell Mol Biol* 41: 348-357, 2009.

26. Hur W, Gray NS. Small molecule modulators of antioxidant response pathway. *Curr Opin Chem Biol* 15: 162-173, 2011.

27. Ivanov AV, Smirnova OA, Ivanova ON, Masalova OV, Kochetkov SN, Isaguliants MG. Hepatitis C virus proteins activate NRF2/ARE pathway by distinct ROS-dependent and independent mechanisms in HUH7 cells. *PLoS ONE* 6: e24957, 2011.

28. Jacoby DB, Choi AM. Influenza virus induces expression of antioxidant genes in human epithelial cells. *Free Radic Biol Med* 16: 821-824, 1994.

29. Jaiswal AK. Nrf2 signaling in coordinated activation of antioxidant gene expression. *Free Radic Biol Med* 36: 1199-1207, 2004.

30. Jamaluddin M, Tian B, Boldogh I, Garofalo RP, Brasier AR. Respiratory syncytial virus infection induces a reactive oxygen species-MSK1-phospho-Ser-276 RelA pathway required for cytokine expression. *J Virol* 83: 10605-10615, 2009.

31. Karin M, Delhase M. The I kappa B kinase (IKK) and NF-kappa B: key elements of proinflammatory signalling. *Semin Immunol* 12: 85-98, 2000.

32. Kaspar JW, Niture SK, Jaiswal AK. Nrf2:INrf2 (Keap1) signaling in oxidative stress. *Free Radic Biol Med* 47: 1304-1309, 2009.

33. Kawai Y, Garduno L, Theodore M, Yang J, Arinze IJ. Acetylation-deacetylation of the transcription factor Nrf2 (nuclear factor erythroid 2-related factor 2) regulates its transcriptional activity and nucleocytoplasmic localization. *J Biol Chem* 286: 7629-7640, 2011.

34. Kesic MJ, Simmons SO, Bauer R, Jaspers I. Nrf2 expression modifies influenza A entry and replication in nasal epithelial cells. *Free Radic Biol Med* 51: 444-453, 2011.

35. Keum YS, Han YH, Liew C, Kim JH, Xu C, Yuan X et al. Induction of heme oxygenase-1 (HO-1) and NAD[P]H: quinone oxidoreductase 1 (NQO1) by a phenolic antioxidant, butylated hydroxyanisole (BHA) and its metabolite, tert-butylhydroquinone (tBHQ) in primary-cultured human and rat hepatocytes. *Pharm Res* 23: 2586-2594, 2006.

36. Khochbin S, Verdel A, Lemercier C, Seigneurin-Berny D. Functional significance of histone deacetylase diversity. *Curr Opin Genet Dev* 11: 162-166, 2001.

37. Kosmider B, Messier EM, Janssen WJ, Nahreini P, Wang J, Hartshorn KL et al. Nrf2 protects human alveolar epithelial cells against injury induced by influenza A virus. *Respir Res* 13: 43, 2012.

38. Lee J, Koh K, Kim YE, Ahn JH, Kim S. Up-regulation of Nrf2 Expression by Human Cytomegalovirus Infection Protects Host Cells from Oxidative Stress. *J Gen Virol* , 94: 1658-1668, 2013.

39. Liu T, Castro S, Brasier AR, Jamaluddin M, Garofalo RP, Casola A. Reactive oxygen species mediate virus-induced STAT activation: role of tyrosine phosphatases. *J Biol Chem* 279: 2461-2469, 2004.

40. Lucidi V, Ciabattoni G, Bella S, Barnes PJ, Montuschi P. Exhaled 8-isoprostane and prostaglandin E(2) in patients with stable and unstable cystic fibrosis. *Free Radic Biol Med* 45: 913-919, 2008.

41. Lupfer C, Patton KM, Pastey MK. Treatment of human respiratory syncytial virus infected Balb/C mice with the proteasome inhibitor bortezomib (Velcade, PS-341) results in increased inflammation and mortality. *Toxicology* 268: 25-30, 2010.

42. MacNee W. Oxidative stress and lung inflammation in airways disease. *Eur J Pharmacol* 429: 195-207, 2001.

43. McKinsey TA. Therapeutic potential for HDAC inhibitors in the heart. *Annu Rev Pharmacol Toxicol* 52: 303-319, 2012.

44. Morcillo EJ, Estrela J, Cortijo J. Oxidative stress and pulmonary inflammation: pharmacological intervention with antioxidants. *Pharmacol Res* 40: 393-404, 1999.

45. Page A, Volchkova VA, Reid SP, Mateo M, Bagnaud-Baule A, Nemirov K et al. Marburgvirus Hijacks Nrf2-Dependent Pathway by Targeting Nrf2-Negative Regulator Keap1. *Cell Rep* , 2014.

46. Patel JA, Kunimoto M, Sim TC, Garofalo R, Eliott T, Baron S et al. Interleukin-1 alpha mediates the enhanced expression of intercellular adhesion molecule-1 in pulmonary epithelial cells infected with respiratory syncytial virus. *Am J Resp Cell Mol* 13: 602-609, 1995.

47. Rahman I, Morrison D, Donaldson K, MacNee W. Systemic oxidative stress in asthma, COPD, and smokers. *Am J Respir Crit Care Med* 154: 1055-1060, 1996.

48. Schaedler S, Krause J, Himmelsbach K, Carvajal-Yepes M, Lieder F, Klingel K et al. Hepatitis B virus induces expression of antioxidant response element-regulated genes by activation of Nrf2. *J Biol Chem* 285: 41074-41086, 2010.

49. Schreiber E, Matthias P, Muller MM, Schaffner W. Rapid detection of octamer binding proteins with 'mini-extracts', prepared from a small number of cells. *Nucleic Acids Res* 17: 6419, 1989.

50. Singh A, Misra V, Thimmulappa RK, Lee H, Ames S, Hoque MO et al. Dysfunctional KEAP1-NRF2 interaction in non-small-cell lung cancer. *PLoS Med* 3: e420, 2006.

51. Spange S, Wagner T, Heinzel T, Kramer OH. Acetylation of non-histone proteins modulates cellular signalling at multiple levels. *Int J Biochem Cell Biol* 41: 185-198, 2009.

52. Sun Z, Chin YE, Zhang DD. Acetylation of Nrf2 by p300/CBP augments promoter-specific DNA binding of Nrf2 during the antioxidant response. *Mol Cell Biol* 29: 2658-2672, 2009.

53. Ueba O. Respiratory syncytial virus: I. concentration and purification of the infectious virus. *Acta Med Okayama* 32: 265-272, 1978.

54. Verdin E, Dequiedt F, Kasler HG. Class II histone deacetylases: versatile regulators. *Trends Genet* 19: 286-293, 2003.

55. Yang XJ, Gregoire S. Class II histone deacetylases: from sequence to function, regulation, and clinical implication. *Mol Cell Biol* 25: 2873-2884, 2005.

56. Zhou LZ, Johnson AP, Rando TA. NF kappa B and AP-1 mediate transcriptional responses to oxidative stress in skeletal muscle cells. *Free Radic Biol Med* 31: 1405-1416, 2001.

FIGURE LEGENDS

Figure 1. RSV infection down-regulates Nrf2 dependent gene transcription. (**A**) Nuclear proteins isolated from A549 cells (left panel) and SAE cells (right panel) uninfected or infected with RSV for 6, 15 and 24h were subjected to western blot analysis using anti-Nrf2 antibody. For loading controls, membranes were stripped and re-probed with anti-Lamin B antibody. The blots are representative of three independent experiments. Densitometric analysis of Nrf2 band intensity is shown after normalization to Lamin B. Data are shown as mean ± SEM. **P* < 0.05 relative to uninfected and 6h infected cells. Open bars represent uninfected (control) and solid bars represent RSV infected cells. (**B**) A549 cells were transiently transfected with an ARE driven luciferase reporter plasmid, infected with RSV for various lengths of time, and harvested to measure luciferase activity. Data are representative of three independent experiments. **P* < 0.05 relative to uninfected and 6h infected cells. The data are representative of three independent experiments and shown as mean ± SEM. **P* < 0.05 relative to uninfected and 6h infected cells. (**C**) ChIP-QgPCR analysis of Nrf2 occupancy of endogenous ARE promoter sites. Chromatin DNA from A549 cells uninfected or infected with RSV for 6, 15 and 24h was immunoprecipitated using anti-Nrf2 antibody or IgG as negative control. QgPCR was performed using primers spanning the ARE binding site of the catalase (left) and SOD1 (right) gene promoter. Total input chromatin DNA for immunoprecipitation was included as positive control for QgPCR amplification. Fold change was calculated compared to IgG control. Data are representative of three independent experiments and are shown as mean ± SEM.**P* < 0.05 relative to uninfected and 6h infected cells.

Figure 2. RSV infection is associated with proteasome-dependent Nrf2 degradation. (**A**) Total cell lysates prepared from A549 cells (left panel) and SAE cells (right panel) uninfected or infected with RSV for 6, 15 and 24h were subjected to Western blot analysis using anti-Nrf2 antibody. For loading controls, membranes were stripped and reprobed using anti-β-Actin antibody. The blots are representative of three independent experiments. Densitometric analysis of Nrf2 band intensity is shown after normalization to β-Actin. Open bars represent uninfected (ctrl) and solid bars represent RSV infected cells. Data are shown as mean ± SEM. **P* < 0.05 relative to uninfected and 6h RSV infected cells. (**B**) Total cell lysates prepared from A549 cells uninfected or infected with RSV for 18h in the presence or absence of 10 μM Lactacystine (Lact) were subjected to Western blot analysis using anti-Nrf2 antibody. For loading controls, membranes were stripped and re-probed with anti-β-Actin antibody. The blots are representative of three independent experiments. Densitometric analysis of Nrf2 band intensity is shown after normalization to β-Actin. Data are shown as mean ± SEM. **P* < 0.05 relative to untreated, RSV infected cells. (**C**) Total cell lysates prepared from A549 cells uninfected or infected with RSV for 18h in the presence or absence of 10 μM Lactacystin and were immunoprecipitated using anti-Nrf2 antibody and immune complexes analyzed by Western blots using anti-ubiquitin antibody. Membrane was stripped and reprobed with anti-Nrf2 antibody to determine the level of immunoprecipitated Nrf2. Lower panel shows Nrf2 Western blot of input of the immunoprecipitation. β-Actin was used as internal control. Blots are representative of three independent experiments.

Figure 3. Blocking Nrf2 degradation rescues ARE-dependent gene expression. (A) A549 cells were transiently transfected with the ARE-luciferase reporter plasmid. Cells uninfected and infected with RSV for 18h in the presence or absence of either 10 μM Lactacystin or MG132 were harvested to measure luciferase activity. Data are representative of three independent experiments and are shown as mean ± SEM. **P* < 0.05 relative to RSV infected, untreated cells. (**B**) A549 cells, uninfected or infected with RSV for 18h in the presence or absence of either 10 μM Lactacystin or MG132, were harvested to prepare total RNA. Catalase (left panel) and SOD1 (right panel) gene expression was quantified by real-time PCR. Data are representative of three independent experiments and are shown as mean ± SEM. **P* < 0.05 relative to RSV infected, untreated cells. (**C**) Chromatin DNA from A549 cells uninfected or infected with RSV for 18h in the presence or absence of either 10 μM Lactacystin or MG132 was immunoprecipitated using anti-Nrf2 antibody or IgG as negative control. QgPCR was performed using primers spanning the ARE binding site of the catalase (left panel) or SOD1 (right panel) gene promoter. Total input chromatin DNA for immunoprecipitation was included as positive control for QgPCR amplification. Fold change was calculated compared to IgG control. Data are representative of three independent experiments and are shown as mean ± SEM. **P* < 0.05 relative to untreated, RSV infected cells.

Figure 4. RSV infection induces Nrf2 deacetylation. (**A**) Total cell lysates from A549 (left panel) and SAE cells (right panel) uninfected or infected with RSV for 15h in the presence or absence of 250 nM TSA were immunoprecipitated using anti-Nrf2 antibody and subjected to Western blot using anti-acetyl lysine antibody. Lower panel shows Nrf2 Western blot for input

of the IP. β-Actin was used as loading control. (**B**) HDAC activity in nuclear extracts prepared from A549 (left panel) and SAE cells (right panel) uninfected and infected with RSV for 6, 15 and 24h was analyzed by using HDAC activity assay kit (Cayman). Data are representative of three independent experiments and are shown as mean ± SEM. **P* < 0.05 relative to uninfected cells. (**C**) Chromatin DNA from A549 cells uninfected or infected with RSV for 6, 15, and 24h was immunoprecipitated using anti-CBP antibody or IgG as negative control. QgPCR was performed using primers spanning the ARE binding site of the SOD1 promoter. Total input chromatin DNA for immunoprecipitation was included as positive control for QgPCR amplification. Fold change was calculated compared to IgG control. Data are representative of three independent experiments and are shown as mean ± SEM. **P* < 0.05 relative to 6h RSV infected cells. (**D**) A549 cells, transiently co-transfected with the ARE-luciferase reporter plasmid and CBP expression plasmid or empty vector (EV), were infected with RSV for 18h and harvested to measure luciferase activity. Data are representative of three independent experiments and are shown as mean ± SEM. **P* < 0.05 relative to EV transfected, RSV infected cells.

Figure 5. Blocking HDAC activity rescues Nrf2-dependent gene transcription. Nuclear protein (**A**) or total cell lysates (**B**) were prepared from A549 cells (left panel) and SAE cells (right panel) uninfected or infected with RSV for 18h in the presence or absence of 250 nM TSA were subjected to Western blot analysis using anti-Nrf2 antibody. For loading controls, membranes were stripped and reprobed using either anti-Lamin B or β-Actin antibody. The blots are representative of three independent experiments. Densitometric analysis of Nrf2 band

intensity is shown after normalization to the appropriate internal control. Data are shown as mean ± SEM. *$P < 0.05$ relative to untreated, RSV infected cells. (**C**) A549 cells were transiently transfected with the ARE-luciferase reporter plasmid. Cells uninfected or infected with RSV for 18h in the presence or absence of 250 nM TSA were harvested to measure luciferase activity. Data are shown as mean ± SEM. *$P < 0.05$ relative to untreated, RSV infected cells. (**D**) A549 cells (upper panel) and SAE cells (lower panel) uninfected or infected with RSV for 18h in the presence or absence of 250 nM TSA were harvested to prepare total RNA. Catalase and SOD1 gene expression was quantified by real-time PCR. Data are representative of three independent experiments and expressed as mean ± SEM. *$P < 0.05$ relative to untreated, RSV infected cells. (**E**) Chromatin DNA from A549 cells uninfected or infected with RSV for 6, 15, and 24h in the presence or absence of 250 nM TSA was immunoprecipitated using an anti-Nrf2 antibody (or IgG as negative control. QgPCR was performed using primers spanning the ARE binding site of the catalase (left) and SOD1 (right) gene promoters. Total input chromatin DNA for immunoprecipitation was included as positive control for QgPCR amplification. Fold change was calculated compared to IgG control. Data are representative of three independent experiments and shown as mean ± SEM. *$P < 0.05$ relative to untreated, RSV infected cells.

Figure 6. Blocking HDAC1 and 2 expression rescues Nrf2 activation. Nuclear protein prepared from A549 cells transfected with nontarget siRNA or (**A**) HDAC1 or (**B**) HDAC2 or (**C**) HDAC3 siRNA, uninfected or infected with RSV for 18h, were subjected to Western blot analysis with anti-Nrf2 antibody. Membranes were stripped and reprobed with anti-HDAC1/2/3 and anti-Lamin B antibodies for loading control. The blots are representative of three

independent experiments. Densitometric analysis of Nrf2 band intensity is shown after normalization to Lamin B. Data are shown as mean ± SEM. *$P < 0.05$ relative to nontarget siRNA transfected, RSV infected cells. (**D**) A549 cells transfected with nontarget siRNA or siRNAs for HDAC1, 2 or 3, uninfected or infected with RSV for 18h, were harvested to prepare total RNA. Catalase (left panel) and SOD1 (right panel) gene expression was quantified by real-time PCR. Data are representative of three independent experiments and are shown as mean ± SEM. *$P < 0.05$ relative to nontarget siRNA transfected, RSV infected cells. (**E**) Chromatin DNA from A549 cells uninfected or infected with RSV for 6 and 15h in the presence or absence of 250 nM TSA was immunoprecipitated using anti-HDAC1 antibody or IgG as negative control. QgPCR was performed using primers spanning the ARE binding site of the SOD1 promoter. Total input chromatin DNA for immunoprecipitation was included as positive control for QgPCR amplification. Fold change was calculated compared to IgG control. Data are representative of three independent experiment and are shown as mean ± SEM. *$P < 0.05$ relative to uninfected cells, **$P < 0.05$ relative to untreated, RSV infected cells.

Figure 7. Nrf2 is deacetylated and degraded through the proteasome pathway *in vivo*. Nuclear protein isolated from lungs of mice that were either sham inoculated (S1-S3) or infected with RSV (R1-R3) for 48h were **(A)** analyzed for HDAC activity by using HDAC activity assay kit. Data are representative of three independent experiments and are shown as mean ± SEM. *$P < 0.05$ relative to sham inoculated mice. **(B)** immunoprecipitated using anti-Nrf2 antibody and subjected to Western blot using anti-acetyl lysine antibody. Lower panel shows Nrf2 Western blot for input of the IP. Lamin B was used as loading control. **(C)** Nuclear protein prepared from

lungs of mice that were either sham inoculated or infected with RSV for 48h in the presence or absence of MG132 were subjected to Western blot analysis using anti-Nrf2 antibody. S1-S3: sham inoculated mice, M1- M3: Sham inoculated, MG132 treated mice, R1-R3: RSV infected mice, and MR1-MR3: MG132 treated, RSV infected mice. For loading controls, membranes were stripped and re-probed with anti-Lamin B antibody. The blots are representative of three independent experiments. Densitometric analysis of Nrf2 band intensity is shown after normalization to Lamin B. Data are shown as mean ± SEM. **P* < 0.05 relative to untreated, RSV infected mice. **(D)** Catalase (left panel) and SOD1 (right panel) gene expression was quantified by q-RT-PCR. Data are representative of three independent experiments and expressed as mean ± SEM. **P* < 0.05 relative to untreated, RSV infected mice.

Figure 8. Nrf2 modulation rescues ARE-dependent gene transcription and ameliorates oxidative stress during RSV infection. (**A**) A549 cells were transiently transfected with the ARE-luciferase reporter plasmid, uninfected or infected with RSV for 18h in the presence or absence of 25μM tBHQ, and harvested to measure luciferase activity. Data are representative of three independent experiments and shown as mean ± SEM. **P* < 0.05 relative to untreated, RSV infected cells. **(B)** SAE cells, uninfected or infected with RSV for 18h in the presence or absence of 25μM tBHQ, were harvested to prepare total RNA. Catalase (left panel) and SOD1 (right panel) gene expression was quantified by real-time PCR. Data are presented as fold changes and are representative of three independent experiments. Data are shown as mean ± SEM. **P* < 0.05 relative to untreated, RSV infected cells. **(C)** SAE cells were infected with RSV for 18h in the presence or absence of 25μM tBHQ. Nuclear protein and total cell lysates were subjected to

Western blot analysis using anti Nrf2 or SOD1 antibodies. For loading controls, membranes were stripped and reprobed using anti Lamin B antibody for nuclear fractions or anti β-Actin antibody for total cell lysates. The blots are representative of three independent experiments. Densitometric analysis of Nrf2 and SOD1 band intensity is shown after normalization to the appropriate internal control. Data are shown as mean ± SEM. *$P < 0.05$ relative to untreated, RSV infected cells. **(D)** Oxidative stress marker 8-isoprostane was measured by competitive enzyme immunoassay from the supernatant of SAE cells uninfected or infected with RSV for 18h in the presence or absence of 25μM tBHQ. Data are representative of three independent experiments and are shown as mean ± SEM. *$P < 0.05$ relative to untreated, RSV infected cells. **(E)** HDAC activity in nuclear extracts prepared from SAE cells uninfected and infected with RSV for 18h in the presence or absence of 25μM tBHQ were analyzed by using HDAC activity assay kit. Data are representative of three independent experiments and are shown as mean ± SEM.

Figure 9. BHA treatment rescues Nrf2 expression and ameliorates oxidative stress *in vivo* during RSV infection. (**A**) Nuclear protein isolated from lungs of mice that were either sham inoculated or infected with RSV for 48h in presence or absence of BHA were subjected to Western blot analysis with anti-Nrf2 antibody. C1-C4: sham inoculated mice, R1-R4: RSV infected mice and B1-B4: BHA treated and RSV infected mice. For loading controls, membranes were stripped and reprobed with anti-Lamin B antibody. The blots are representative of three independent experiments. Densitometric analysis of Nrf2 band intensity is shown after normalization to Lamin B. Data are shown as mean ± SEM. *$P < 0.05$ relative to untreated, RSV

infected mice. (**B**) Catalase (left panel) and SOD1 (right panel) gene expression was quantified by q-RT-PCR. Data are representative of three independent experiments and shown as mean ± SEM. **P* < 0.05 relative to untreated, RSV infected mice. (**C**) Oxidative stress marker 8-isoprostane was measured by competitive enzyme immunoassay in BAL of mice sham inoculated or infected with RSV for 48h in the presence or absence of BHA. Data are representative of three independent experiments and are shown as mean ± SEM. **P* < 0.05 relative to untreated, RSV infected mice.

ROLE OF HYDROGEN SULFIDE IN PARAMYXOVIRUS INFECTIONS

Hui Li[1], Yinghong Ma[1], Teodora Ivanciuc[1], Narayana Komaravelli[1], John P. Kelley[1], Ciro Coletta[2], Csaba Szabo[2], Roberto P. Garofalo[1,3,4], Antonella Casola[1,3,4#]

Departments of Pediatrics[1], Department of Anesthesiology[2], Sealy Centers for Vaccine Development[3] and for Molecular Medicine[4], University of Texas Medical Branch at Galveston, TX, USA

Running Head: RSV and H_2S

#Address correspondence to: Antonella Casola, M.D., ancasola@utmb.edu; University of Texas Medical Branch at Galveston, Galveston, TX, USA

Abstract word count: 246

Manuscript word count: 5,386

ABSTRACT

Hydrogen sulfide (H_2S) is a novel gaseous mediator that has gained increasing recognition as an important player in modulating acute and chronic inflammatory diseases. However, its role in viral-induced lung inflammation is currently unknown. Respiratory syncytial virus (RSV) is a major cause of upper and lower respiratory tract infections in children, for which no vaccine or effective treatment is available. Using the slow-releasing H_2S donor GYY4137 and propargylglysin (PAG), an inhibitor of cystathionine-γ-lyase (CSE), a key enzyme that produce intracellular H_2S, we found that RSV infection led to reduced ability to generate and maintain intracellular H_2S levels in airway epithelial cells (AECs). Inhibition of CSE with PAG resulted in increased viral replication and chemokine secretion. On the other hand, treatment of AECs with the H_2S donor GYY4137 reduced proinflammatory mediator production and significantly reduced viral replication, even when administered several hours after viral absorption. GYY4137 also significantly reduced replication and inflammatory chemokine production induced by human metapneumovirus (hMPV), suggesting a broad inhibitory effect of H_2S administration on paramyxovirus replication. GYY4137 treatment had no effect on RSV genome replication, viral mRNA and protein synthesis, indicating that the inhibition occurs at the level of assembly and/or cellular release. GYY4137 inhibition of proinflammatory gene expression occurred by modulation of activation of the key transcription factors Nuclear Factor (NF)-κB and Interferon Regulatory Factor (IRF)-3. Our results underscore an important role of H_2S in regulating virus infection and host defenses that could lead to a novel treatment strategy for RSV infection.

IMPORTANCE

RSV is a global health concern, causing significant morbidity, and economic losses, as well as mortality in developing countries. After decades of intensive research, no vaccine or treatment is available for this infection, as well as for other important respiratory mucosal viruses. This study identifies hydrogen sulfide as a novel cellular mediator that can modulate viral replication and proinflammatory gene expression, both important determinants of lung injury in respiratory viral infections, with potential for rapid translation of such finding into novel therapeutic approaches for viral bronchiolitis and pneumonia.

INTRODUCTION

Hydrogen sulfide (H_2S) is an endogenous gaseous transmitter which participates in the regulation of the respiratory system's physiological functions and pathophysiological alterations, such as chronic obstructive pulmonary disease, asthma, pulmonary fibrosis and hypoxia-induced pulmonary hypertension, as it regulates lung functions such as airway constriction, pulmonary circulation, cell proliferation/apoptosis, fibrosis, oxidative stress, and inflammation [reviewed in (1)]. H_2S is produced endogenously in mammals, including humans, by three enzymes: cystathionine-γ-lyase (CSE), cystathionine-β-synthase (CBS), and 3-mercaptopyruvate sulfurtransferase (MST)(2-4). Sulfide salts such as sodium hydrosulfide (NaHS) and sodium sulfide (Na_2S) have been widely used to study the biological effects of hydrogen sulfide in many cells, tissues and animals. These salts generate a large burst of H_2S over a short time period, when used in cell culture. GYY4137 is a novel water-soluble H_2S donor that releases H_2S slowly over a period of hours (5). H_2S donors have been used to demonstrate how therapeutic H_2S administration exert significant effects in various animal models of inflammation, reperfusion injury and circulatory shock (6). There are no studies investigating the role of H_2S generation in pathophysiology of viral infections or the use of H_2S donors as pharmacological intervention for viral-induced diseases.

Respiratory tract infections are a leading cause of morbidity and mortality worldwide. Paramyxoviruses, which include respiratory syncytial virus (RSV) and human metapneumovirus (hMPV), represent a major cause of pediatric upper and lower respiratory tract infections (7,8). They are associated with bronchiolitis, pneumonia and flu-like syndromes, as well as asthma exacerbations, and represent a substantial public health problem for the community. No vaccine or treatment is available for either RSV or hMPV. Our previous studies have shown that both

viruses induce the expression of a variety of proinflammatory genes, including cytokine and chemokines in airway epithelial cells (AECs), the main target of infection (9,10), which are likely to play a major role in disease pathogenesis. Cytokine and chemokine gene expression in viral-infected cells is orchestrated by activation of two key transcription factors, nuclear factor (NF)-κB and interferon regulatory factor (IRF)-3. A number of viral-inducible inflammatory and immunoregulatory genes require NF-κB for their transcription and/or are dependent on an intact NF-κB signaling pathway (11,12), and IRF-3 is necessary for viral induction of RANTES transcription and gene expression (13,14).

To start addressing the role of H_2S generation/administration in viral infections, we used an *in vitro* model of RSV infection of AECs. We found that RSV infection led to decreased expression of CSE and reduced ability to generate cellular H_2S, as well as increased H_2S degradation. Inhibition of H_2S generation, using PAG, was associated with increased generation of virus infectious particles, as well as increased proinflammatory mediator secretion, suggesting an important role of endogenous H_2S in controlling viral replication. GYY4137 treatment of both A549 (a lung carcinoma cell line retaining features of type II alveolar epithelial cells) and primary small alveolar epithelial (SAE) cells significantly reduced viral-induced proinflammatory mediators release and it significantly inhibited viral replication at a step subsequent to viral adsorption. GYY4137 administration blocked RSV replication without significant reducing viral mRNA synthesis, viral genome replication and viral protein synthesis, indicating that it affects steps involved in viral assembly and/or release.

GYY4137 treatment of AECs infected with RSV did not affect the initial step of viral-induced activation of IRF-3 and NF-κB, as shown by no changes in their nuclear translocation, however, it did significantly reduced IRF-3 and NF-κB binding to the endogenous promoter of

proinflammatory genes, resulting in inhibition of chemokine gene transcription, indicating an important effect of H_2S on cellular signaling.

MATERIALS AND METHODS

Materials. GYY4137 (morpholin-4-ium 4 methoxyphenyl(morpholino) phosphinodithioate), a novel water-soluble, slow-releasing H_2S compound and DL-Propargyl Glysin (PAG), an inhibitor of H_2S generating enzyme cystathionine-γ-lyase (CSE), were purchased from Sigma-Aldrich company (Sigma, St. Louis, MO, USA). Solutions were prepared freshly in culture medium and filtered through 0.2μm filter before treatment. Sulfidefluor-7 acetoxymethyl ester (SF7-AM), a fluorescent probes that allows direct, real-time visualization of endogenous H_2S produced in live human cells (15), was generously provided by Dr. Christopher J. Chang, (Department of Chemistry, University of California, Berkeley). SF7-AM stock solution was prepared in DMSO and diluted in serum free medium at least a thousand fold.

Virus preparation. The RSV Long strain was grown in Hep-2 cells and purified by centrifugation on discontinuous sucrose gradients, as described (16,17), and viral pools were titered in plaque forming units (PFU)/mL using a methylcellulose plaque assay, as described (18). No contaminating cytokines or LPS, tested by the limulus hemocyanin agglutination assay, were found in these viral preparations. Virus pools were aliquoted, quick-frozen on dry ice/alcohol and stored at -80^{o}C until used.

The hMPV strain CAN97-83 was obtained from the Centers for Disease Control (CDC), Atlanta, GA, with permission from Dr. Guy Boivin at the Research Center in Infectious Diseases, Regional Virology Laboratory, Laval University, Quebec City, Canada, propagated on

LLC-MK2 cells and purified on sucrose cushions, as previously described (19). Virus pools were titered in PFU/ml by immunostaining, as previously described (19).

Cell culture and viral infection. A549 cells, a human alveolar type II-like epithelial cell line (American Type Culture Collection, Manassas, VA) and small alveolar epithelial (SAE) cells (Clonetics, San Diego, CA), derived from terminal bronchioli of cadaveric donors, were grown in F12K and small airway epithelial cell (SAEC) growth medium respectively, containing 10% (vol/vol) FBS, 10 mM glutamine, 100 IU/mL penicillin and 100 µg/mL streptomycin for F12K medium, and 7.5 mg/mL bovine pituitary extract (BPE), 0.5 mg/mL hydrocortisone, 0.5 µg/mL hEGF, 0.5 mg/mL epinephrine, 10 mg/mL transferrin, 5 mg/mL insulin, 0.1 µg/mL retinoic acid, 0.5 µg/mL triiodothyronine, 50 mg/mL gentamicin and 50 mg/mL bovine serum albumin (BSA) for SAE medium. When SAE were used for RSV-infection, they were changed to basal medium, not supplemented with growth factors, 6h prior to and throughout the length of the experiment. Confluent cell monolayers were infected with RSV or hMPV at multiplicity of infection (MOI) of 1, as previously described (20), unless otherwise stated. For GYY4137 and PAG experiments, cells were seeded into 24-well plates, infected with RSV or hMPV for 1h at 37°C and 5% CO_2, and then treated with GYY4137 or PAG after viral inoculum was removed.

Methylene blue assay. H_2S production was measured by colorimetric methylene blue assay, as previously described (21). Briefly, cells were homogenized and incubated at 37°C for 5 min then cooled down on ice for 10 min. L-cysteine (1 and 3 mmol/L) and pyridoxal 5-phosphate (2 mmol/L) were added and incubated for 1h at 37° C. 1% zinc acetate and 10% trichloroacetic acid

solution were used to terminate the reaction. After adding N,N-dimethylphenylendiamine sulfate and $FeCl_3$ for 15 min, optical absorbance of the solutions was measured at 650 nm.

SF7-AM fluorescence assay. A549 cells were grown in eight-well Lab-Tek II glass chamber slides (Thermo Scientific, Pittsburgh, USA) and incubated with 5μM SF7-AM probe at 37^0C for 30 min. After washing with culture medium, A549 cells were infected with RSV and treated with GYY4137, as described above. Confocal fluorescence imaging studies were performed with a Zeiss laser scanning microscope 710 with a 20× water objective lens, with Zen 2009 software (Carl Zeiss). SF7-AM was excited using a 488 nm Argon laser, and emission was collected using a META detector between 500 and 650 nm. Cells were imaged at 37°C and 5% CO_2 throughout the course of the experiment. Image analysis was performed using Metamorph software (Carl Zeiss), and fluorescence was quantified by using the mean pixel intensity after setting a common threshold for all images.

Luciferase Assay. A549 cells were transiently transfected using a NF-κB- or ISRE-driven luciferase reporter plasmid, containing five repeats of the NF-κB site of the IgG promoter or three repeats of the RANTES ISRE promoter, respectively, linked to the luciferase reporter gene, using Fugene 6 (Roche Diagnostic Corp., Indianapolis, Ind.), as previously described (22)(14). 0.5 μg of the reporter gene plasmid and 0.05 μg of β-galactosidase expression plasmid/well were premixed with FuGene 6 and added to the cells in regular medium. The next day, cells were infected with RSV for 1h, followed by treatment with GYY4137 and harvested at either 15 or 24 h post-infection (p.i.) to independently measure luciferase and β-galactosidase reporter activity,

as previously described (22). Luciferase activity was normalized to the internal control β-galactosidase activity. Results are expressed in arbitrary units.

Determination of lactate dehydrogenase activity. Lactate dehydrogenase (LDH) activity in the medium, an index of cellular damage, was measured by colorimetric assay using a commercially available kit (Cayman Chemical. MI, USA) following manufacturer's instructions.

Quantitative real-time PCR. Total RNA was extracted using ToTALLY RNA kit from Ambion (Cat # AM1910, Austin, TX). RNA samples were quantified using a Nanodrop Spectrophotometer (Thermo Fisher Scientific Inc., Wilmington, DE), and quality was analyzed on RNA Nano or Pico chip using the Agilent 2100 Bioanalyzer (Agilent Technologies). Synthesis of cDNA was performed with 1 µg of total RNA in a 20-µl reaction using the Taqman Reverse Transcription Reagents Kit from ABI (Applied Biosystems, cat. #N8080234). The reaction conditions were as follows: 25 °C 10 min, 48 °C 30 min, 95 °C 5 min. Quantitative real-time PCR amplification (performed in triplicate) was done with 1 µl of cDNA in a total volume of 25 µl using the Faststart Universal SYBR Green Master Mix (Roche Applied Science cat. #04913850001). The final concentration of the primers was 300 nM. 18S RNA was used as housekeeping gene for normalization. PCR assays were run in the ABI Prism 7500 Sequence Detection System with the following conditions: 50 °C 2 min, 95 °C 10 min and then 95 °C 15 s, 60 °C 1 min for 40 cycles. RSV N-specific RT primer contained a tag sequence from the bacterial chloroamphenicol resistance gene to generate the cDNA, because of self-priming exhibited by RSV RNA. Duplicate cycle threshold (CT) values were analyzed in Microsoft Excel

by the comparative CT (ΔΔCT) method as described by the manufacturer (Applied Biosystems). The amount of target ($2^{-\Delta\Delta CT}$) was obtained by normalizing to endogenous reference (18S) sample. To detect RSV N transcript, we used RSV N dT+Tag (RT primer): CTGCGATGAGTGGCAGGCTTTTTTTTTTTTAACTY-AAAGCTC Cmr Tag. For PCR assay, RSV Tag (R primer): CTGCGATGAGTGGCAGGC. RSV N forward primer: ACTACAGTGT-ATTAGACTTRACAGCAGAAG. To detect genome (-) strand, we used RSV N+Tag F (RT primer): 5' CTGCGATGAGTGGCAGGCACTACAGTGTATTAGACTTRA-CAGCAGAAG 3' Cmr Tag. For PCR assay, RSV Tag: CTGCGATGAGTGGCAGGC. RSV P R#2 primer: GCATCTTCTCCATGRAATTCAGG.

Western blotting. Nuclear extracts of uninfected and infected cells were prepared using hypotonic/nonionic detergent lysis, according to Schreiber protocol (23). To prevent contamination with cytoplasmic proteins, isolated nuclei were purified by centrifugation through 1.7 M sucrose buffer for 30 min, at 12,000 rpm, before nuclear protein extraction, as previously described (24). Total cell lysates were prepared from uninfected and infected A549 cells by adding ice-cold lysis buffer (50 mM Tric-HCl, pH 7.4, 150 mM NaCl, 1mM EGTA, 0.25% sodium deoxycholate, 1 mM Na_3VO_4, 1 mM NaF, 1% Triton X-100 and 1 μg/ml of aprotinin, leupeptin and pepstatin). After incubation on ice for 10 min, the lysates were collected and detergent insoluble materials were removed by centrifugation at 4° C at 14,000 g. Proteins (10 to 20 μg per sample) were then boiled in 2X Laemmli buffer and resolved on SDS-PAGE. Proteins were transferred onto Hybond-polyvinylidene difluoride membrane (Amersham, Piscataway, NJ) and nonspecific binding sites were blocked by immersing the membrane in Tris-buffered saline-Tween (TBST) containing 5% skim milk powder or 5% bovine serum albumin

for 30 min. After a short wash in TBST, membranes were incubated with the primary antibody for 1h at room temperature or overnight at 4° C, depending on the antibody used, followed by HRP-conjugated secondary antibody (Sigma, St. Louis, MO, diluted 1:10,000 in TBST for 30 min at room temperature. After washing, proteins were detected using an enhanced chemiluminescence system (RPN 2016, Amersham, GE Healthcare, UK) and visualized through autoradiography. Antibodies used for Western blot assay were goat anti-RSV polyclonal antibody from Ab D SeroTec, rabbit anti-p65, anti-Ser536 or -Ser276 p65, from Cell Signaling Technology, Inc, Danvers, MA, and rabbit anti-IRF-3, from Santa Cruz Biotechnology, Santa Cruz, CA.

Bio-Plex. Cell-free supernatants were tested for multiple cytokines and chemokines using the Bio-Plex Cytokine Human Multi-Plex panel (Bio-Rad Laboratories, Hercules, CA), according to the manufacturer's instructions. IL-8 and RANTES were also quantified by enzyme-linked immunosorbent assay (ELISA) following the manufacturer's protocol (DuoSet R&D Systems, Minneapolis, MN).

Chromatin immunoprecipitation (ChIP) and quantitative genomic PCR (Q-gPCR). For ChIP assays, we used ChIP-IT Express kit from Active Motif (Carlsbad, CA), following manufacturer instruction with some modifications. Briefly, A549 cells in 10 cm plate were washed three times with PBS and fixed with freshly prepared 2mM disuccinimidyl gluterate (DSG) for 45 min at room temperature. After three washes with PBS, cells were fixed with freshly prepared formaldehyde for 10 min and neutralized with glycine for 5 min at room temperature. Cells were harvested and disrupted using a dounce homogenizer to isolate nuclei. Nuclei were sheared by

sonication to obtain DNA fragments from 200 to 1500 base pair. Twenty micrograms of sheared chromatin were immunoprecipitated with 5 μg of ChIP grade anti-NF-κB (sc-722X) or -IRF-3 antibodies (sc-369X) from Santa Cruz Biotechnology, CA, USA, and magnetic beads conjugated with protein G at 4° C overnight. Immunoprecipitation with IgG antibody was used as negative control. Chromatin was reverse crosslinked, eluted from magnetic beads, and purified using Qiagen PCR purification kit (Qiagen, USA). Q-gPCR was done by SyBR green based real-time PCR using the following primers spanning the IL-8 gene NF-κB promoter site: forward-AGGTTTGCCCTGAGGGGATG and reverse- GGAGTGCTCCGGTGGCTTTT, or the RANTES gene ISRE promoter site: forward-AGCGGCTTCCTGCTCTCTGA and reverse-CAGCTCAGGCTGGCCCTTTA. Total input chromatin DNA for immunoprecipitation was included as positive control for PCR amplification.

In vivo efficacy of GYY4137. 10-12 week-old BALB/c mice were purchased from Harlan (Houston, TX) and were housed in pathogen-free conditions in the animal research facility of the University Texas Medical Branch (UTMB), Galveston, Texas, in accordance with the National Institutes of Health and UTMB institutional guidelines for animal care. Under light anesthesia, mice were inoculated intranasally (i.n.) with 10^6 PFU of sucrose-purified RSV in a final volume of 50 μl/dose diluted in phosphate buffered saline (PBS). Control animals (mock infected), receiving PBS, were treated in a similar manner. Mice were given i.n. GYY4137 (50 mg/kg body weight) or an appropriate volume of vehicle (PBS) 1h before, 6 and 24h after infection. Mice from all groups were evaluated daily for body weight loss over the experimental period. These parameters have been shown to closely correlate with lung pathology in experimental paramyxovirus infection of BALB/c mice (25). At day 5 p.i., infected animals were sacrificed,

lungs were excised, snap-frozen in liquid nitrogen, and stored at -80° C. Viral titers were determined by plaque assay and expressed as PFU/gram of lung tissue.

Statistical analysis. Statistical analyses were performed with the InStat 3.05 Biostatistics Package from GraphPad, San Diego, CA. To ascertain differences between two groups, student's t Test was used and if more than two groups were compared, one-way analysis of variance was performed. Values of $p<0.05$ were considered statistically significant. Unless otherwise indicated, values for all measurements are expressed as the mean ± SEM in the figures.

RESULTS

RSV infection affects H_2S generation in airway epithelial cells. H_2S is an endogenous gaseous transmitter which participates in the regulation of the respiratory system's physiological functions and pathophysiological alterations (1). Among the three H_2S generating enzymes CSE, CBS and MST, CSE represents the major source of H_2S in lung tissue and it uses cysteine as the main substrate. Sulfide:quinone oxidoreductase (SQOR) is a membrane-bound enzyme that catalyzes the first step in the mitochondrial metabolism of H_2S (26). To determine whether RSV induced changes in H_2S generating and metabolizing enzymes in AECs, A549 cells were infected for 6, 15 and 24h, and harvested to extract total RNA and measure CSE, CBS and SQOR mRNA levels by real-time PCR. We found that CSE expression was decreased by RSV infection at later time points (Fig.1A), while there was no significant change in CBS or MST mRNA level (data not shown). On the other hand, there was a significant time-dependent increase in SQOR mRNA expression in RSV-infected cells, compared to uninfected (Fig.1B). To investigate whether RSV modulated the capacity of airway epithelial cells to generate H_2S, A549

276 cells were infected for 15h and harvested to prepare total cell lysates. H_2S production was then
277 measured by methylene blue assay. There was a significant reduction in H_2S generation in RSV-
278 infected cells, compared to uninfected, when cysteine was supplied at 1 and 3mM concentration
279 as CSE substrate (Fig.1C). When A549 cells were treated with the slow-releasing H_2S donor
280 GYY4137, there was a significant increase in intracellular levels of H_2S, detected by the
281 fluorescent probe SF-7AM, which was significantly lower in infected cells, suggesting an
282 increase in H_2S degradation following RSV infection (Fig.1D).
283
284 *CSE inhibition enhances RSV-induced chemokine production and viral replication.* To examine
285 the effect of CSE inhibition on viral-induced cellular responses, A549 cells were infected with
286 RSV for one hour and then treated with different concentrations of DL-propargylglycine (PAG).
287 Cell supernatants were harvested at 24h p.i. to measure viral-induced chemokine secretion. PAG
288 administration significantly increased RANTES and IL-8 production in response to RSV
289 infection in dose dependent manner (Fig.2A). PAG treatment of A549 cells also resulted in a
290 significant increase in viral infectious particle formation, assessed by plaque assay (Fig.2B),
291 indicating a role of endogenous H_2S production in viral replication and proinflammatory cellular
292 responses.
293
294 *Effects of H_2S treatment on RSV-induced proinflammatory mediator production.* To investigate
295 the effect of increasing intracellular H_2S level on viral responses, we determined levels of
296 cytokine and chemokine secretion in A549 cells infected with RSV in the presence or absence of
297 GYY4137, a slow-releasing H_2S donor. A549 cells were infected with RSV for one hour,
298 followed by incubation with different concentrations of GYY4137, and harvested to collect cell

supernatant at 24h p.i. to measure proinflammatory mediator release by ELISA and Bio-Plex assays. As show in Fig.3A, RSV-induced secretion of several cytokines and chemokines, such as IL-6 and IL-8, RANTES, macrophage inflammatory protein-1β, and interferon-induced protein-10, was decreased by GYY4137 treatment in a dose-dependent manner. To investigate possible GYY4137 cytotoxicity, supernatants of A549 cells uninfected and infected, treated and untreated, were harvested and tested for LDH release. There was no enhanced cellular damage, but on the contrary protection against viral-induced cytotoxicity, in response to GYY4137 treatment (Fig.3B). Inhibition of proinflammatory secretion, following RSV infection, by GYY4137 administration was also confirmed in SAE cells, normal human AECs derived from cadaveric donor, which we have shown to behave very similarly to A549 cells in terms of chemokine/cytokine gene expression, transcription factor and signaling pathway activation, after RSV infection (10,17,20,27-30)(Fig.4).

Effects of H_2S treatment on RSV replication. To determine whether increasing intracellular H_2S levels would affect viral replication, A549 cells were infected with RSV for one hour, treated with different GYY4137 concentrations and harvested at 24 p.i. to measure viral titer by plaque assay. There was a significant decrease in RSV replication, in particular with the highest dose of the H_2S donor, in the order of several log reduction (Fig.5), indicating a significant antiviral activity of H_2S administration. To investigate whether this effect was reproducible if GYY4137 was administered several hours after infection, A549 cells were treated at 3 and 6h p.i. and harvested to measure viral titer. We observed a significant decrease in RSV replication with both treatments, although somewhat less striking when compared to the 1h p.i. administration (Fig.5), indicating that GYY4137 can affect viral replication when infection is already well established.

322

323 *H_2S treatment affects viral particle release.* To further investigate how H_2S treatment affected
324 viral replication, we used several approaches, including quantification of viral gene transcription,
325 genome replication, viral antigen detection and viral particle release. GYY4137 administration
326 did not decrease the number of RSV genome copies and N gene copies, on the contrary they
327 were somewhat increased at the all concentrations tested (Fig.6A and B). Viral protein
328 expression, assessed by Western blot assay of total cell lysates, was not significantly affected by
329 GYY4137 treatment at any of the dose tested (Fig.6C). When viral titers were assessed
330 separately on cell supernatants and cell pellets, we found that GYY4137 administration
331 dramatically reduced the number of infectious virus present in the cell supernatant, with a much
332 less robust effect on the one associated with the cell pellet (Fig.6D, left versus right panel),
333 suggesting that H_2S treatment affects viral replication in part at the level of virus assembly but
334 mostly at the level of virus release.

335

336 *Effect of GYY4137 on RSV-induced cellular signaling.* Cytokine and chemokine gene expression
337 in A549 cells infected by RSV is orchestrated by activation of the two key transcription factors
338 NF-κB and IRF-3. To determine whether changes in RSV-induced cytokine and chemokine
339 production observed with GYY4137 treatment affected NF-κB and IRF-3 dependent gene
340 transcription, we performed reporter gene assays. Cells were transiently transfected with either a
341 NF-κB- or IRF-driven luciferase reporter plasmid and then were treated with GYY4137 after 1h
342 of viral adsorption and harvested at 24 h p.i. to measure luciferase activity. RSV infection
343 significantly enhanced both IRF-3 and NF-κB-dependent gene transcription, which was

significantly inhibited by the GYY4137 treatment in a dose-dependent manner (Fig.7A and B), consistent with the reduction observed in IL-8 and RANTES secretion.

To determine whether GYY4137 treatment was able to modulate viral-induced NF-κB and IRF-3 activation, A549 cells were infected with RSV for 1hr, incubated with or without GYY4137 and harvested at 15 and 24h p.i. to prepare either total cell lysates or nuclear extracts. NF-κB and IRF-3 nuclear levels or cellular levels of serine phosphorylated p65, the major NF-κB subunit activated in response to RSV infection (20), were assessed by Western blot. Nuclear translocation of both transcription factors was not changed by GYY4137 treatment, compared to RSV infection alone (Fig.7C), however, there was a significant decrease in RSV-induced p65 Ser276 and Ser536 phosphorylation (Fig.7D), two important post-translational modifications that affect NF-κB transcriptional activity (31). In addition, GYY4137 treatment significantly reduced p65 and IRF- occupancy of their cognate binding site on the IL-8 and RANTES endogenous promoter, assessed by a two-step chromatin immunoprecipitation (XChIP) and genomic PCR (Q-gPCR) assay (Fig.7E).

Taken together, these results indicate that increasing cellular H_2S by a slow-releasing donor can effectively modulate the strong pro-inflammatory cellular response induced by RSV infection through blocking IRF- and NF-κB-dependent gene transcription.

Effects of H_2S treatment on hMPV-induced chemokine production and viral replication. To investigate whether GYY4137 had a similar antiviral and anti-inflammatory effect on other paramyxoviruses, we measured chemokine secretion and viral replication in A549 cells in response to hMPV infection. A549 cells were infected with hMPV for one hour and incubated in the presence or absence of GYY4137 for a total of 24h. Cell supernatants were collected to

measure levels of IL8 and RANTES induction by ELISA, while viral titers were determined by immunostaining. As shown in Fig.8A, hMPV-induced IL-8 and RANTES secretion was significantly decreased by GYY4137 treatment in a dose-dependent manner. Similarly, viral replication was also significantly reduced by GYY4137, as shown in Fig.8B. These results suggest that GYY4137 might have a broad antiviral effect on paramyxoviruses.

Effects of H_2S treatment in vivo. Finally, we examined the impact of GYY4137 treatment on viral infection *in vivo*, by measuring viral replication and body weight loss in a well-established model of RSV infection. In this mouse model, RSV viral replication can be detected around day 3 p.i., peaks at day 5 and is cleared by day 7 p.i. (32). As shown in Fig. 9A, intranasal delivery of GYY4137 to RSV-inoculated mice significantly reduced peak of viral replication, compared to mock-treated, RSV-infected mice. To determine whether H_2S donor administration was capable of altering RSV-induced disease, we assessed the effect of GYY4137 treatment on body weight loss. Mice were treated i.n. with GYY4137 or an appropriate volume of vehicle and body weight was measured for the following week. As shown in Fig. 9B, mice treated with PBS and infected with RSV progressively lost weight during the first 2 days of infection, with a peak of loss at day 2 p.i. GYY4137 treatment significantly attenuated RSV-induced body weight loss, as the mice experienced less weight loss at day 2 p.i. and a faster recovery to reach baseline body weight (Fig. 9B), indicating that H_2S donor administration can modulate RSV-induced clinical disease.

DISCUSSION

In this study we investigated the role of H_2S in airway epithelial cell responses to viral infection. Paramyxoviruses, in particular RSV and hMPV, are a primary cause of severe lower respiratory

tract infections in children, as well as in other populations, leading to increased morbidity and mortality, for which there is no vaccine or treatment, beside supportive measures. The viral-induced lung inflammatory response, triggered by secretion of cytokine and chemokine from viral-infected airway resident cells, such as AECs and alveolar macrophages, plays an important role in disease pathogenesis. We and others have shown that modulation of the inflammatory response is associated with amelioration of clinical illness in animal models of RSV infection (33-36), making it an important target for the development of effective treatment strategies.

H_2S is an important endogenous gaseous mediator that has been recently the focus of intense investigation, leading to supportive evidence that it plays an important role in vasoactive, cytoprotective, anti-inflammatory and antioxidant cellular responses [reviewed in (37)]. Our study shows for the first time that H_2S has a protective role in RSV infection by modulating both inflammatory gene expression and viral replication. AECs infected with RSV displayed a decreased ability to generate H_2S and enhanced degradation of H_2S released by the donor GYY4137, indicating that viral infection leads to changes in H_2S cellular homeostasis. Endogenous H_2S production appears to play an important role in modulating viral-induced chemokine secretion and viral replication, as both were significantly enhanced by treatment of AECs with the CSE inhibitor PAG, while increased H_2S cellular levels, as a result of administration of GYY4137, were associated with a significant reduction of proinflammatory mediator production and most importantly a striking reduction in viral replication.

GYY4137 administration resulted in a strong inhibition of viral replication at a step subsequent to viral adsorption. It dramatically reduced the amount of infectious virus present in the cell supernatant, with a much less robust effect on cell-associated virus, without having a significant effect on viral gene transcription, protein synthesis, or genome replication. These

findings suggest that H_2S treatment inhibits viral replication in part at the level of virus assembly, but mostly at the level of virus release, which in part explain the increase in cellular viral mRNA and genomic RNA levels observed with H_2S treatment. To produce progeny virions, ribonuclear protein complexes, which form cytoplasmic inclusions and contain the newly synthesized genomic RNA together with several viral proteins translated in the cytoplasm, have to be assembled with the surface glycoproteins that have trafficked to the cell surface through the secretory pathway and then released to form mature infectious virus [reviewed in (38)]. The apical recycling endosome (ARE) has been implicated in RSV protein trafficking and membrane scission, and downregulation of specific proteins such as myosin Vb or Rab11 disrupt virion formation and result in diminished viral progeny. To date, it is not known whether H_2S, or any other endogenous gaseous transmitters, modulates ARE functions. The final step in viral assembly and budding involves a membrane scission event to separate the assembled viral particle from the host cell membrane, which often involves the multivesicular body formation and endosomal sorting complex required for transport (ESCRT) protein system, with membrane scission performed by the ATPase Vps4 (38). In RSV case, budding is unaffected by inhibition of Vps4, suggesting that RSV uses a novel mechanism for this final step of replication. Some evidence suggests that surface glycoproteins could actively contribute to the budding process leading to RSV egression from infected cells (38). Although we did not detect significant changes in the level of expression of most viral proteins, including the glycoprotein G, we have not investigated whether H_2S treatment could affect their routing to the cell membrane.

Endogenous H_2S production and exogenous H_2S administration have been associated to both pro-inflammatory and anti-inflammatory effects in various models of disease [reviewed in (39)]. In the context of acute pancreatitis and in burn injury, for example, H_2S seems to play a

436 pro-inflammatory role, while in other pathologies such as asthma, COPD, LPS-induced
437 inflammation, and ischemia reperfusion it displays anti-inflammatory properties. In models of
438 lung injury, administration of H_2S donors has been often associated with an anti-inflammatory
439 effect. For example, in a mouse model of hyperoxia, treatment with NaHS was associated with
440 reduced lung permeability and inflammation, due to decreased production of proinflammatory
441 mediators such as IL-1β, MCP-1, and MIP-2, and increased anti-inflammatory cytokine
442 expression (40). Similar results were obtained in other models of acute lung injury, such as the
443 one associated with hemorrhagic shock or with bleomycin treatment (41,42).
444 Recent studies have established that H_2S is indeed a biologically relevant signaling
445 molecule, similar to the other gaseous mediator nitric oxide and carbon monoxide [reviewed in
446 (43)]. In several models of inflammatory diseases, the inhibition of proinflammatory mediator
447 expression was paralleled by the inhibition of NF-κB activation. NaHS administration inhibited
448 NF-κB activation in a mouse model of hemorrhagic shock, as well as in a rat ALI model of lung
449 inflammation. Similarly, H_2S donor treatment in a rat model of bleomycin-induced pulmonary
450 inflammation and fibrosis led to inhibition of activation of the NF-κB subunit p65 (44). *In vitro*,
451 NaHS and GYY4137 have been shown to inhibit LPS-induced NF-κB activation in cultured
452 macrophages (5). Garlic compounds such as diallyl sulfide, a possible H_2S donor, can also
453 downregulate NF-κB activation (41). GYY4137 treatment of AECs infected with RSV did not
454 change primary viral-induced activation of IRF-3 and NF-κB, as shown by no changes in their
455 nuclear translocation, in agreement with no differences due to GYY4137 treatment in viral RNA
456 generation, the major trigger of cellular signaling in RSV-infected cells through activation of the
457 viral sensing cytosolic receptor RIG-I (45). GYY4137 treatment, however, did significantly
458 reduced IRF-3 and NF-κB binding to RANTES and IL-8 endogenous promoters, indicating a

459 direct effect of H_2S on cellular signaling. An important mechanism by which H_2S can modulate
460 cellular signaling is through its direct and indirect antioxidant activity (reviewed in (43)).
461 Administration of H_2S has been shown to increase cellular glutathione levels and it has also been
462 associated with increased activation of Nrf2, a transcription factor that regulates oxidative stress
463 by affecting gene expression of several key antioxidant enzymes (43). Inducible phosphorylation
464 on distinct serine residues, including Ser276 and Ser536, has been shown to regulate NF-κB
465 transcriptional activity without modification of nuclear translocation or DNA-binding affinity
466 (31). We have recently shown that inhibition of RSV-induced reactive oxygen species (ROS)
467 formation by treatment of AECs with antioxidants significantly reduces RSV-dependent NF-κB
468 serine phosphorylation, resulting in the inhibition of RSV-induced expression of several NF-κB-
469 dependent genes, without affecting nuclear translocation (46). Our finding that H_2S treatment
470 significantly reduced p65 Ser276 and Ser536 phosphorylation suggest that modulation of ROS
471 cellular levels could be a major mechanism by which H_2S affects viral-induced cellular
472 signaling.

473 In conclusion, we have shown that modulation of cellular H_2S significantly impacts
474 cellular responses and viral replication in an *in vitro* model of RSV infection. Our finding that
475 H_2S donor treatment affects hMPV replication and hMPV-induced proinflammatory mediator
476 production as well suggests that H_2S could possess a broad antiviral activity. We are currently
477 investigating the effect of H_2S donors in the context other paramyxo and non-paramyxovirus
478 infection to test this possibility. We are also determining the role of the enzymes CSE and CBS
479 in RSV infection *in vivo*, taking advantage of knock-out mice available for each of these two
480 enzymes. Indeed, preliminary studies indicate that CSE is an important modulator of airway
481 hyperresponsiveness triggered by RSV infection (Casola A, personal communication), similar to

what recently reported for allergic airway inflammation triggered by ovalbumin sensitization in mice (47). Of interest is the observation that premature infants, who are at high risk of developing severe bronchiolitis following RSV and other respiratory viral infections, have very low tissue CSE activity compared to full-term infants (48). We are also evaluating the efficacy of H_2S donors in a mouse model of RSV infection, to determine whether their administration has therapeutic potential for prevention and treatment of viral-induced lung disease.

ACKNOWLEDGMENTS

This project was supported by R01 AI062885, P01 AI07924602, GM107846, P30ES006676 and W81XWH1010146-DoD. The authors would like to thank Kimberly Palkowetz and Tianshuang Liu for technical assistance and Cynthia Tribble for manuscript submission.

REFERENCES

1. Chen, Y. and R. Wang. 2012. The message in the air: Hydrogen sulfide metabolism in chronic respiratory diseases. Respiratory Physiology & Neurobiology 184:130-138.
2. Wang, P., G. Zhang, T. Wondimu, B. Ross, and R. Wang. 2011. Hydrogen sulfide and asthma. Experimental Physiology 96:847-852.
3. Wang, R. 2012. Physiological implications of hydrogen sulfide: a whiff exploration that blossomed. Physiol Rev. 92:791-896. doi:92/2/791 [pii];10.1152/physrev.00017.2011 [doi].
4. Wang, R. 2011. Signaling pathways for the vascular effects of hydrogen sulfide. Curr.Opin.Nephrol.Hypertens. 20:107-112. doi:10.1097/MNH.0b013e3283430651 [doi].

5. Li, L., M. Whiteman, Y. Y. Guan, K. L. Neo, Y. Cheng, S. W. Lee, Y. Zhao, R. Baskar, C. H. Tan, and P. K. Moore. 2008. Characterization of a novel, water-soluble hydrogen sulfide-releasing molecule (GYY4137): new insights into the biology of hydrogen sulfide1. Circulation 117:2351-2360. doi:CIRCULATIONAHA.107.753467 [pii];10.1161/CIRCULATIONAHA.107.753467 [doi].
6. Szabo, C. 2007. Hydrogen sulphide and its therapeutic potential. Nat.Rev.Drug Discov. 6:917-935. doi:nrd2425 [pii];10.1038/nrd2425 [doi].
7. Hall, C. B., G. A. Weinberg, M. K. Iwane, A. K. Blumkin, K. M. Edwards, M. A. Staat, P. Auinger, M. R. Griffin, K. A. Poehling, D. Erdman, C. G. Grijalva, Y. Zhu, and P. Szilagyi. 2009. The burden of respiratory syncytial virus infection in young children. N.Engl.J.Med. 360:588-598.
8. Williams, J. V., P. A. Harris, S. J. Tollefson, L. L. Halburnt-Rush, J. M. Pingsterhaus, K. M. Edwards, P. F. Wright, and J. E. Crowe, Jr. 2004. Human metapneumovirus and lower respiratory tract disease in otherwise healthy infants and children. N.Engl.J Med. 350:443-450.
9. Garofalo, R. P. and H. Haeberle. 2000. Epithelial regulation of innate immunity to respiratory syncytial virus. Am J Respir Cell Mol Biol 23:581-585.
10. Bao, X., T. Liu, L. Spetch, D. Kolli, R. P. Garofalo, and A. Casola. 2007. Airway epithelial cell response to human metapneumovirus infection. Virology 368:91-101.
11. Bitko, V., A. Velazquez, L. Yank, Y.-C. Yang, and S. Barik. 1997. Transcriptional induction of multiple cytokines by human respiratory syncytial virus requires activation of NF-kB and is inhibited by sodium salicylate and aspirin. Virology 232:369-378.

12. Tian B, Zhang Y, B. Luxon, R. P. Garofalo, A. Casola, M. Sinha, and Brasier A.R. 2002. Identification of NF-kB dependent gene networks in respiratory syncytial virus-infected cells. J Virol 76:6800-6814.
13. Lin, R., C. Heylbroeck, P. Genin, P. M. Pitha, and J. Hiscott. 1999. Essential role of interferon regulatory factor 3 in direct activation of RANTES chemokine transcription. Molec Cellular Biol 19:959-966.
14. Casola, A., R. P. Garofalo, H. Haeberle, T. F. Elliott, A. Lin, M. Jamaluddin, and Brasier A.R. 2001. Multiple *cis* regulatory elements control RANTES promoter activity in alveolar epithelial cells infected with respiratory syncytial virus. J Virol 75:6428-6439.
15. Lin, V. S., A. R. Lippert, and C. J. Chang. 2013. Cell-trappable fluorescent probes for endogenous hydrogen sulfide signaling and imaging H2O2-dependent H2S production. Proc.Natl.Acad.Sci.U.S.A 110:7131-7135. doi:1302193110 [pii];10.1073/pnas.1302193110 [doi].
16. Ueba, O. 1978. Respiratory syncytial virus: I. concentration and purification of the infectious virus. Acta.Med.Okayama 32:265-272.
17. Olszewska-Pazdrak, B., A. Casola, T. Saito, R. Alam, S. E. Crowe, F. Mei, P. L. Ogra, and R. P. Garofalo. 1998. Cell-specific expression of RANTES, MCP-1, and MIP-1alpha by lower airway epithelial cells and eosinophils infected with respiratory syncytial virus. J Virol 72:4756-4764.
18. Kisch, A. L. and K. M. Johnson. 1963. A plaque assay for respiratory syncytial virus. Proc.Soc.Exp.Biol.Med. 112:583.
19. Kolli, D., X. Bao, T. Liu, C. Hong, T. Wang, R. P. Garofalo, and A. Casola. 2011. Human metapneumovirus glycoprotein G inhibits TLR4-dependent signaling in

monocyte-derived dendritic cells. J.Immunol. 187:47-54. doi:jimmunol.1002589 [pii];10.4049/jimmunol.1002589 [doi].

20. Garofalo, R. P., M. Sabry, M. Jamaluddin, R. K. Yu, A. Casola, P. L. Ogra, and A. R. Brasier. 1996. Transcriptional activation of the interleukin-8 gene by respiratory syncytial virus infection in alveolar epithelial cells: Nuclear translocation of the RelA transcription factor as a mechanism producing airway mucosal inflammation. J Virol 70:8773-8781.

21. Asimakopoulou, A., P. Panopoulos, C. T. Chasapis, C. Coletta, Z. Zhou, G. Cirino, A. Giannis, C. Szabo, G. A. Spyroulias, and A. Papapetropoulos. 2013. Selectivity of commonly used pharmacological inhibitors for cystathionine beta synthase (CBS) and cystathionine gamma lyase (CSE). Br.J.Pharmacol. 169:922-932. doi:10.1111/bph.12171 [doi].

22. Casola, A., R. P. Garofalo, M. Jamaluddin, S. Vlahopoulos, and A. R. Brasier. 2000. Requirement of a novel upstream response element in RSV induction of interleukin-8 gene expression: stimulus-specific differences with cytokine activation. J.Immunol. 164:5944-5951.

23. Schreiber, E., P. Matthias, M. M. Muller, and W. Schaffner. 1989. Rapid detection of octamer binding proteins with 'mini-extracts', prepared from a small number of cells. Nucleic Acids Res. 17:6419.

24. Brasier, A. R., H. Spratt, Z. Wu, I. Boldogh, Y. Zhang, R. P. Garofal, A. Casola, J. Pashmi, A. Haag, B. Luxon, and A. Kurosky. 2004. Nuclear Heat Shock Response and Novel Nuclear Domain 10 Reogranization in Respiratory Syncytial Virus-Infected A549 Cells identified By High Resolution 2D Gel Electrophoresis. J Virol 78:11461-11476.

25. Graham, B. S., M. D. Perkins, P. F. Wright, and D. T. Karzon. 1988. Primary respiratory syncytial virus infection in mice. J.Med.Virol. 26:153-162.

26. Jackson, M. R., S. L. Melideo, and M. S. Jorns. 2012. Human sulfide:quinone oxidoreductase catalyzes the first step in hydrogen sulfide metabolism and produces a sulfane sulfur metabolite. Biochemistry 51:6804-6815. doi:10.1021/bi300778t [doi].

27. Casola, A., N. Burger, T. Liu, M. Jamaluddin, Brasier A.R., and R. P. Garofal. 2001. Oxidant tone regulates RANTES gene transcription in airway epithelial cells infected with Respiratory Syncytial Virus: role in viral-induced Interferon Regulatory Factor activation. J Biol Chem. 276:19715-19722.

28. Zhang Y, B. Luxon, A. Casola, R. P. Garofalo, M. Jamaluddin, and Brasier A.R. 2001. Expression of RSV-induced chemokine gene networks in lower airway epithelial cells revealed by cDNA microarrays. J Virol 75:9044-9058.

29. Pazdrak, K., B. Olszewska-Pazdrak, B. Liu, R. Takizawa, A. R. Brasier, R. P. Garofalo, and A. Casola. 2002. MAP-kinase activation is involved in post-transcriptional regulation of RSV-induced RANTES gene expression. Am J Physiol000.

30. Hosakote, Y. M., Jantzi, P. D., Esham, D. L., Spratt, H., Kurosky, A., Casola, A., and Garofalo, R. P. Viral-mediated inhibition of antioxidant enzymes contributes to the pathogenesis of severe respiratory syncytial virus bronchiolitis. Am J Respir Crit Care

31. Zhong, H., R. E. Voll, and S. Ghosh. 1998. Phosphorylation of NF-kappa B p65 by PKA stimulates transcriptional activity by promoting a novel bivalent interaction with the coactivator CBP/p300. Molecular Cell 1:661-671.

32. Kolli, D., M. R. Gupta, E. Sbrana, T. S. Velayutham, C. Hong, A. Casola, and R. P. Garofalo. 2014. Alveolar Macrophages Contribute to the Pathogenesis of hMPV

595 Infection While Protecting Against RSV Infection. Am.J.Respir.Cell Mol.Biol.
596 doi:10.1165/rcmb.2013-0414OC [doi].
597 33. Haeberle, H. A., W. A. Kuziel, H. J. Dieterich, A. Casola, Z. Gatalica, and R. P.
598 Garofalo. 2001. Inducible expression of inflammatory chemokines in respiratory
599 syncytial virus-infected mice: role of MIP-1alpha in lung pathology. J Virol 75:878-890.
600 34. Haeberle, H. A., A. Casola, Z. Gatalica, S. Petronella, H. J. Dieterich, P. B. Ernst, A. R.
601 Brasier, and R. P. Garofalo. 2004. IkappaB Kinase Is a Critical Regulator of Chemokine
602 Expression and Lung Inflammation in Respiratory Syncytial Virus Infection. J.Virol.
603 78:2232-2241.
604 35. Bennett, B. L., R. P. Garofalo, S. G. Cron, Y. M. Hosakote, R. L. Atmar, C. G. Macias,
605 and P. A. Piedra. 2007. Immunopathogenesis of respiratory syncytial virus bronchiolitis.
606 J Infect.Dis. 195:1532-1540.
607 36. Castro, S. M., A. Guerrero-Plata, G. Suarez-Real, P. A. Adegboyega, G. N. Colasurdo, A.
608 M. Khan, R. P. Garofalo, and A. Casola. 2006. Antioxidant Treatment Ameliorates
609 Respiratory Syncytial Virus-induced Disease and Lung Inflammation. Am.J.Respir.Crit
610 Care Med. 174:1361-1369.
611 37. Kimura, H. 2014. Production and physiological effects of hydrogen sulfide.
612 Antioxid.Redox.Signal. 20:783-793. doi:10.1089/ars.2013.5309 [doi].
613 38. El, N. F., A. P. Schmitt, and R. E. Dutch. 2014. Paramyxovirus Glycoprotein
614 Incorporation, Assembly and Budding: A Three Way Dance for Infectious Particle
615 Production. Viruses. 6:3019-3054. doi:v6083019 [pii];10.3390/v6083019 [doi].

39. Whiteman, M. and P. G. Winyard. 2011. Hydrogen sulfide and inflammation: the good, the bad, the ugly and the promising. Expert.Rev.Clin.Pharmacol. 4:13-32. doi:10.1586/ecp.10.134 [doi].

40. Li, H. D., Z. R. Zhang, Q. X. Zhang, Z. C. Qin, D. M. He, and J. S. Chen. 2013. Treatment with exogenous hydrogen sulfide attenuates hyperoxia-induced acute lung injury in mice. Eur.J.Appl.Physiol 113:1555-1563. doi:10.1007/s00421-012-2584-5 [doi].

41. Kalayarasan, S., N. Sriram, and G. Sudhandiran. 2008. Diallyl sulfide attenuates bleomycin-induced pulmonary fibrosis: critical role of iNOS, NF-kappaB, TNF-alpha and IL-1beta. Life Sci. 82:1142-1153. doi:S0024-3205(08)00131-8 [pii];10.1016/j.lfs.2008.03.018 [doi].

42. Xu, D. Q., C. Gao, W. Niu, Y. Li, Y. X. Wang, C. J. Gao, Q. Ding, L. N. Yao, W. Chai, and Z. C. Li. 2013. Sodium hydrosulfide alleviates lung inflammation and cell apoptosis following resuscitated hemorrhagic shock in rats. Acta Pharmacol.Sin. 34:1515-1525. doi:aps201396 [pii];10.1038/aps.2013.96 [doi].

43. Li, L., P. Rose, and P. K. Moore. 2011. Hydrogen sulfide and cell signaling. Annu.Rev.Pharmacol.Toxicol. 51:169-187. doi:10.1146/annurev-pharmtox-010510-100505 [doi].

44. Cao, H., X. Zhou, J. Zhang, X. Huang, Y. Zhai, X. Zhang, and L. Chu. 2014. Hydrogen sulfide protects against bleomycin-induced pulmonary fibrosis in rats by inhibiting NF-kappaB expression and regulating Th1/Th2 balance. Toxicol.Lett. 224:387-394. doi:S0378-4274(13)01414-8 [pii];10.1016/j.toxlet.2013.11.008 [doi].

45. Liu, P., M. Jamaluddin, K. Li, R. P. Garofalo, A. Casola, and A. R. Brasier. 2007. Retinoic Acid-inducible gene I mediates early antiviral response and toll-like receptor 3

639 expression in respiratory syncytial virus-infected airway epithelial cells. J.Virol. 81:1401-
640 1411.
641 46. Jamaluddin, M., B. Tian, I. Boldogh, R. P. Garofalo, and A. R. Brasier. 2009. Respiratory
642 syncytial virus infection induces a reactive oxygen species-MSK1-phospho-Ser-276 RelA
643 pathway required for cytokine expression. J.Virol. 83:10605-10615.
644 47. Benetti, L. R., D. Campos, S. A. Gurgueira, A. E. Vercesi, C. E. Guedes, K. L. Santos, J.
645 L. Wallace, S. A. Teixeira, J. Florenzano, S. K. Costa, M. N. Muscara, and H. H.
646 Ferreira. 2013. Hydrogen sulfide inhibits oxidative stress in lungs from allergic mice in
647 vivo. Eur.J.Pharmacol. 698:463-469. doi:S0014-2999(12)00956-9
648 [pii];10.1016/j.ejphar.2012.11.025 [doi].
649 48. Vina, J., M. Vento, F. Garcia-Sala, I. R. Puertes, E. Gasco, J. Sastre, M. Asensi, and F. V.
650 Pallardo. 1995. L-cysteine and glutathione metabolism are impaired in premature infants
651 due to cystathionase deficiency. Am.J.Clin.Nutr. 61:1067-1069.
652

FIGURE LEGENDS

FIG. 1. Effect of RSV infection on H_2S production in airway epithelial cells. A549 cells were infected with RSV for 6, 15 and 24h, and harvested to prepare total RNA. CSE (**A**) and SQOR (**C**) mRNA levels in uninfected and RSV-infected cells were measured by qRT-PCR. Results are representative of two independent experiments run in duplicate. * $P<0.05$, compared to uninfected cells. (**B**) A549 cells were infected with RSV for 15h and harvested to prepare total cell lysates. H_2S production in uninfected and RSV-infected cells was determined by methylene blue colorimetric assay. Results are representative of three independent experiments. * $P<0.05$, compared to uninfected cells. (**D**) A549 cells were incubated with 5μM fluorescent probe SF-7AM and infected with RSV for 1h. Medium or 10mM GYY4137 was added to uninfected or infected cells and incubated for 15h. Left panel shows images of cells uninfected, untreated (control) and 10 mM GYY4137 treated, uninfected or infected cells. Right panel shows average fluorescent intensity quantified by confocal microscopy using the Zeiss Metamorph software. * $P<0.05$, compared to uninfected, treated cells.

FIG. 2. Effect of CSE inhibition on RSV-induced cytokine and chemokine production and viral replication. A549 cells were infected with RSV for 1h and then incubated in the presence or absence of 20 or 40 mM PAG. (**A**) Cell supernatants from uninfected and RSV-infected, treated or untreated, were assayed at 24h p.i. for cytokine and chemokine secretion by ELISA. Results are expressed as mean ± standard error. Results are representative of two independent experiments run in triplicate. (**B**) Cells were treated as in (A) and harvested at 24h p.i.to determine viral titers by plaque assay. * $P<0.05$, compared to untreated RSV-infected cells.

FIG. 3. Effect of H_2S donor treatment on RSV-induced cytokine and chemokine production in A549 cells. Cells were infected with RSV for 1h and then incubated in the presence or absence of GYY4137 at 1, 5 and 10mM for 24h. Cell supernatants were assayed for (**A**) cytokine and chemokine secretion by ELISA or Bio-Plex, and (**B**) cytotoxicity by LDH release assay. Results are expressed as mean ± standard error and are representative of two to three independent experiments run in triplicate. * $P<0.05$, compared to untreated RSV-infected cells.

FIG. 4. Effect of H_2S donor treatment on RSV-induced cytokine and chemokine production in SAE cells. Cells were infected with RSV for 1h and then incubated in the presence or absence of GYY4137 at 5 and 10mM for 24h. Cell supernatants were assayed for cytokine and chemokine secretion by ELISA or Bio-Plex. Results are expressed as mean ± standard error and are representative of two to three independent experiments run in triplicate. * $P<0.05$, compared to untreated RSV-infected cells.

FIG. 5. Effect of H_2S donor treatment on RSV replication. A549 cells were infected with RSV for either 1, 3 or 6h and then incubated in the presence or absence of GYY4137 at 5 and 10mM for 24h. Cells were harvested to determine viral titer by plaque assay. Results are expressed as mean ± standard error and are representative of two to three independent experiments run in triplicate. * $P<0.05$, compared to untreated RSV-infected cells.

FIG. 6. Effect of H_2S donor treatment on different steps of viral replication. A549 cells were infected with RSV for 1h and then incubated in the presence or absence of GYY4137 for 24h.

699 Cells were harvested to prepare either total RNA to measure (**A**) viral genome copies or (**B**) RSV
700 N gene copies by qRT-PCR, or (**C**) total cell lysates to measure viral protein expression Western
701 blot. Membrane was stripped and reprobed with β-actin as a control for equal loading of the
702 samples. Figures are representative of two independent experiments with similar results. (**D**)
703 A549 cells were infected with RSV for either 1h and then incubated in the presence or absence
704 of GYY4137 at 5 and 10mM for 24h. Cell supernatants (left panel) and cell pellets (right panel)
705 were harvested separately to determine viral titer by plaque assay. Results are expressed as mean
706 ± standard error and are representative of two independent experiments run in triplicate. *
707 $P<0.05$, compared to untreated RSV-infected cells.
708
709 **FIG. 7. Effect of H_2S donor treatment on viral-induced signaling.** A549 cells were
710 transiently transfected with an ISRE- (**A**) or NF-κB-driven (**B**) reporter gene plasmid, infected
711 with RSV for 1h and then treated with 5 and 10 mM GYY4137. Cells were harvested at 15 or 24
712 h p.i. to measure luciferase and β-galactosidase reporter activity. Luciferase was normalized to
713 the internal control β-galactosidase activity. Results are representative of two independent
714 experiments run in triplicate. Data are expressed as mean ± standard error of normalized
715 luciferase activity. * $P< 0.05$ relative to untreated, RSV-infected cells. (**C**) A549 cells were
716 infected with RSV for 1h, followed by GYY4137 treatment at different concentration, and
717 harvested at 15 and 24h p.i. to prepare either total cell lysates or nuclear extracts. IRF-3 and p65
718 nuclear translocation was assessed by Western blot of nuclear extracts. Membranes were stripped
719 and reprobed with Lamin B to determine equal loading of the samples. (**D**) Total Ser276 and
720 Ser536 p65 phosphorylation levels were detected by Western blot of total cell lysates. Membrane
721 was stripped and reprobed for total p65 and β-actin to determine equal loading of the samples.

Figures are representative of two independent experiments with similar results. (**E**) Chromatin DNA from A549 cells uninfected and RSV infected in the presence or absence of with GYY4137 for 15h was immunoprecipitated using an anti-NF-κB antibody (left panel) or anti-IRF-3 antibody (right panel) or IgG as negative control. QgPCR was performed using primers spanning either the NF-κB binding site of the IL-8 promoter or the ISRE binding site of the RANTES promoter. Total input chromatin DNA for immunoprecipitation was included as positive control for QgPCR amplification. Fold change was calculated compared to IgG control. Data are representative of three independent experiments. *P<0.05 relative to untreated, RSV infected cells.

FIG. 8. Effect of H_2S donor treatment on hMPV-induced chemokine production and viral replication. A549 cells were infected with hMPV for 1h followed by treatment with different mM concentrations of GYY4137. (**A**) Cell supernatants from uninfected and hMPV-infected, treated or untreated, were assayed at 24h p.i. for RANTES and IL8 secretion by ELISA. Results are expressed as mean ± standard error. Results are representative of two independent experiments run in triplicate. * P<0.05 compared to untreated RSV-infected cells. (**B**) Viral replication was determined 24h post infection by titration of viral infectious particles released in the cell supernatants by plaque assay. Results are representative of two independent experiments run in triplicate. * P<0.05 compared to untreated RSV-infected cells.

FIG. 9. H_2S donor treatment attenuates RSV-induced clinical disease and viral replication in vivo. (**A**) Viral replication in the lungs. At day 5 p.i., lungs were excised and viral replication was determined by plaque assay. The bar graph represents mean ± standard error (n = 4

745 mice/group).*p<0.01 compared with PBS/RSV group. (**B**) Disease parameters. Mice were
746 treated i.n. with GYY4137 (50 mg/kg body weight) or an appropriate volume of vehicle (PBS)
747 1h before, 6 and 24h after infection. Mice were inoculated with RSV dose 10^6 PFU. Data are
748 expressed as mean ± standard error (n = 4 mice/group) and is representative of two independent
749 experiments. *p<0.01 compared with PBS/RSV at day 2 p.i., **p<0.05 compared with PBS/RSV
750 at days 3, 4, and 5 p.i.